sequence, as shown by in vitro cleavage reactions. However, in contrast to the specificity, suppression of mutant SOD1 protein expression by them in the mammalian cells was much lower than that obtained with siRNA G93A under the conditions used in our investigation.

Two possible explanations may account for such a big difference in efficiency between siRNA and DNA enzyme/ribozyme at codon 93. First, double-stranded siRNAs are protected by proteins in cells from attacks by ribonucleases, whereas single-stranded RNA/DNA are not, as demonstrated earlier [11]. Second, the secondary structure of SOD1 mRNA at this site might not be accessible by ribozyme or DNA enzyme. The secondary structure of target RNA highly influences the efficiencies of ribozyme and DNA enzyme, but not that of siRNA [4,5,16], probably because, in some step of siRNA, ATP-dependent RNA helicase may unwind duplex RNA [9,17]. Therefore, we also compared the ribozyme, DNA enzyme, and siRNA that were designed to target the largest single-strand region of SOD1 ORF mRNA with minimal free energy predicted by the mFold program of Zuker. Actually, Rz405 and Dz398 cleaved most of the in vitro-transcribed full-length SOD1 RNA in 4 h, with efficiencies that were much better than those for Rz G93X and Dz G93A, and were comparable to or even better than those of reported constructs [18,19]. For the ribozyme expression in the cells, furthermore, an internally cleaved hairpin ribozyme cassette was inserted downstream of the hammerhead ribozyme to remove 3′ extraneous sequences, which may interfere with ribozyme activity [13,20]. Rz405, as well as Dz398 was, however, still much less efficient in the cells than siRNA396.

It is a very important result for the gene therapy of congenital disease that siRNA396 could efficiently suppress endogenous SOD1 expression. Considering the facts that the half-life of SOD1 protein is a few days and that transfection efficiency of siRNA was 80–90% (judging by the result of the control GFP plasmid), a 60–70% reduction of total endogenous SOD1 by siRNA396 (Fig. 3C) suggests nearly complete elimination of endogenous SOD1 expression in the successfully transfected cells. In contrast, neither Rz405 nor Dz398 was effective in suppressing endogenous SOD1 expression. Therefore, the current studies would suggest that siRNA is clearly a potent and promising tool for silencing of the target gene in cells.

Although our non-specific siRNAs do not discriminate between mutant and wild-type SOD1 mRNAs, it is possible that a reduction in expression of both mutant and wild-type SOD1 may also be beneficial for rescue of the phenotype. There are several lines of evidences suggesting that reduction of wild-type SOD1 activity will not produce or enhance the phenotype of motor neuron loss. First, in ALS patients with SOD1 mutations neither the age of onset nor the rapidity of progression of disease correlates with SOD1 activity level [15]. Although the downregulation of SOD1 may cause neuronal death in cultured cells [21], SOD1 null mice developed normally without motor neuron disease [22]. More importantly, elimination of wild-type endogenous SOD1 by crossing G85R SOD1 transgenic mice with SOD1 null mice was found to have no effect on mutant-mediated disease [23]. These observations suggest the possibility that reduction of mutant proteins, even if it is accompanied by the reduction of wild-type SOD1 to a similar degree, may be sufficient for improving the phenotype. In our cell line model, indeed, siRNA396, which suppressed expression of both mutant and wild-type SOD1, rescued the enhanced cell toxicity produced by overexpression of G93A and A4V SOD1s.

For the application of the siRNA approach to gene therapy of neurodegenerative disease in vivo, we must develop a way to achieve long-term expression of siRNA in post-mitotic neurons (and possibly glia, as well). siRNA therapy, like antisense DNA and DNA enzyme therapies, requires continuous delivery of sufficient quantities of therapeutic molecules to inhibit translation of target mRNA. In contrast, ribozyme encoded in recombinant adeno-associated viruses (rAAVs) can be incorporated in the host chromosomal DNA in neurons and transcribed indefinitely [24]. Therefore, in order to use a viral delivery system for siRNA, we tried vector-mediated expression of siRNA. We constructed a DNA-based siRNA expression vector in which each sense and antisense siRNA sequence was placed under control of human U6 promoter with a termination signal at the 3′ end (short stretch of uridines). Expressed stem-loop transcript would be cleaved by endogenous Dicer and form siRNA duplexes with two 3′ overhangs in the cells. All of the expressing vectors of siRNA G93A.1, G93A.2, and 396 worked well, i.e., to the similar degree to siRNA of oligonucleotides in cells. We are in the process of making rAAV and transgenic mice expressing siRNA396 and G93A.2 for investigating the efficacy of siRNAs in vivo. Although a less-invasive delivery method for introducing in vivo cells is needed for clinical feasibility, the efficiency of our siRNA and expressing RNA vector to reduce mutant SOD1 protein in cells suggests that this mRNA-targeting approach by siRNA might provide effective therapy for autosomal dominant disease, such as familial ALS.

Acknowledgments

The authors thank Alyson Peel, Ph.D., Dr. Li Yi, Dr. Hiroki Sasaguri. and Dr. Yuki Saito for their help. This study was supported by Grants from the National Institutes of Health (NS35155 to D.E.B.) and the ALS Association, the Ministry of Education, Science and Culture, Japan (A-130, T.Y.), from the Ministry of Health, Labor and Welfare, Japan (T.Y., H.M.), and from Japan Amyotrophic Lateral Sclerosis Association (T.Y.).

References

[1] D.R. Rosen, T. Siddique, D. Patterson, D.A. Figlewicz, P. Sapp, A. Hentati, D. Donaldson, J. Goto, J.P. O'Regan, H.X. Deng, Mutations in Cu, Zn superoxide dismutase are associated with familial amyotrophic lateral sclerosis, Nature 362 (1993) 59–66.

[2] D.W. Cleveland, From Charcot to SOD1: mechanisms of selective motor neuron death in ALS, Neuron 24 (1983) 515–520.

[3] C. Baglioni, T.W. Nilsen, Mechanisms of antiviral action of interferon, Interferon 5 (1999) 23–42.

[4] B.R. Williams, Role of the double-stranded RNA-activated protein kinase (PKR) in cell regulation, Biochem. Soc. Trans. 25 (1997) 509–513.

[5] S.M. Elbashir, J. Harborth, W. Lendeckel, A. Yalcin, K. Weber, T. Tuschl, Duplexes of 21-nucleotide RNAs mediate RNA interference in cultured mammalian cells, Nature 411 (2001) 494–498.

[6] S.M. Elbashir, J. Martinez, A. Patkaniowska, W. Lendeckel, T. Tuschl, Functional anatomy of siRNAs for mediating efficient RNAi in *Drosophila melanogaster* embryo lysate, EMBO J. 20 (2001) 6877–6888.

[7] D.E. Ruffer, G.D. Stormo, O.C. Uhlenbeck, The sequence requirements of the hammerhead self-cleavage reaction, Biochemistry 29 (1990) 10695–10702.

[8] S.W. Santoro, G.F. Joyce, A general purpose RNA-cleaving DNA enzyme, Proc. Natl. Acad. Sci. USA 94 (1997) 4262–4266.

[9] P.A. Sharp, RNA interference, Genes Dev. 15 (2001) 485–490.

[10] T.R. Brummelkamp, R. Bernards, R. Agami, A system for stable expression of short interfering RNAs in mammalian cells, Science 296 (2002) 550–553.

[11] M. Miyagishi, K. Taira, U6 promotor-driven siRNAs with four urideine 3′ overhangs efficiently suppress targeted gene expression in mammalian cells, Nat. Biotechnol. 19 (2002) 497–500.

[12] J. Ohkawa, K. Taira, Control of the functional activity of an antisense RNA by a tetracycline-responsive derivative of the human U6 snRNA promoter, Hum. Gene Ther. 11 (2000) 577–585.

[13] M. Altschuler, R. Tritz, A. Hampel, A method for generating transcripts with defined 5′ and 3′ termini by autolytic processing, Gene 122 (1992) 85–90.

[14] H.B. Oral, C.V. Arancibia-Carcamo, D.O. Haskard, A.J. George, A method for determining the cytoprotective effect of catalase in transiently transfected cell lines and in corneal tissue, Anal. Biochem. 267 (1999) 196–202.

[15] A. Radunovic, P.N. Leigh, Cu/Zn superoxide dismutase gene mutations in amyotrophic lateral sclerosis: correlation between genotype and clinical features, J. Neurol. Neurosurg. Psychiatry 61 (1996) 565–572.

[16] T. Holen, M. Amarzguioui, M. Wiiger, E. Babaie, H. Prydz, Positional effects of short interfering RNAs targeting the human coagulation trigger tissue factor, Nucleic Acids Res. 30 (2002) 1757–1766.

[17] T. Dalmay, R. Horsefield, T.H. Braunstein, D.C. Baulcombe, SDE3 encodes an RNA helicase required for post-transcriptional gene silencing in *Arabidopsis*, EMBO J. 20 (2001) 2069–2078.

[18] M. Warashina, T. Kuwabara, Y. Nakamatsu, K. Taira, Extremely high and specific activity of DNA enzymes in cells with a Philadelphia chromosome, Chem. Biol. 6 (1999) 237–250.

[19] F.S. Santiago, H.C. Lowe, M.M. Kavurma, C.N. Chesterman, A. Baker, D.G. Atkins, L.M. Khachigian, New DNA enzyme targeting Egr-1 mRNA inhibits vascular smooth muscle proliferation and regrowth after injury, Nat. Med. 5 (1999) 1264–1269.

[20] J. Ohkawa, N. Yuyama, Y. Takebe, S. Nishikawa, K. Taira, Importance of independence in ribozyme reactions: kinetic behavior of trimmed and of simply connected multiple ribozymes with potential activity against human immunodeficiency virus, Proc. Natl. Acad. Sci. USA 90 (1993) 11302–11306.

[21] J.D. Rothstein, L.A. Bristrol, B. Hosler, R.H. Brown, R.W. Kuncl, Chronic inhibition of superoxide dismutase produces apoptotic death of spinal neurons, Proc. Natl. Acad. Sci. USA 91 (1994) 4155–4159.

[22] A.G. Reaume, J.L. Elliott, E.K. Hoffman, N.W. Kowall, R.J. Ferrante, D.F. Siwek, H.M. Wilcox, D.G. Flood, M.F. Beal, R.H. Brown Jr., Motor neurons in Cu/Zn superoxide dismutase-deficient mice develop normally but exhibit enhanced cell death after axonal injury, Nat. Genet. 13 (1996) 43–47.

[23] L.I. Bruijn, M.K. Houseweart, S. Kato, K.L. Anderson, S.D. Anderson, E. Ohama, A.G. Reaume, R.W. Scott, D.W. Cleveland, Aggregation and motor neuron toxicity of an ALS-linked SOD1 mutant independent from wild-type SOD1, Science 281 (1998) 1851–1854.

[24] A.S. Lewin, K.A. Drenser, W.W. Hauswirth, S. Nishikawa, D. Yasumura, J.G. Flannery, M.M. LaVail, Ribozyme rescue of photoreceptor cells in a transgenic rat model of autosomal dominant retinitis pigmentosa, Nat. Med. 4 (1998) 967–971.

Sequence-Dependent and Independent Inhibition Specific for Mutant Ataxin-3 by Small Interfering RNA

Yi Li, MD,[1] Takanori Yokota, MD,[1]
Ryusuke Matsumura, MD,[2] Kazunari Taira, PhD,[3]
and Hidehiro Mizusawa, MD[1]

In Machado–Joseph disease (MJD) gene, there is a C/G polymorphism immediately after the CAG repeat; the expanded CAG repeat tract is exclusively followed by C, whereas about half of wild-type alleles are followed by G. Using this C/G polymorphism, we have engineered the small interfering RNA (siRNA) which decreased the expression of mutant ataxin-3, Q79C, by 96.0%, whereas there was minimal reduction on that of the wild type, Q22G (5.9%). Furthermore, unexpectedly, the expression of another wild-type allele, Q22C, was also much less suppressed (22.5%) by this siRNA possibly due to difference of the secondary structure of the target RNA. This is the first report of sequence-independent discrimination of mutant and wild-type alleles by siRNA.

Ann Neurol 2004;56:124–129

From the [1]Department of Neurology and Neurological Science, Graduate School, Tokyo Medical and Dental University, Tokyo; [2]Department of Neurology, Nara Medical University, Nara; [3]Department of Chemistry and Biotechnology, School of Engineering, University of Tokyo, Tokyo, Japan.

Received Nov 24, 2003, and in revised form Feb 25, 2004. Accepted for publication Apr 2, 2004.

Published online Jun 28, 2004, in Wiley InterScience (www.interscience.wiley.com). DOI: 10.1002/ana.20141

Address correspondence to Dr Yokota, Department of Neurology, Tokyo Medical and Dental University, 1-5-45 Yushima, Bunkyo-ku, Tokyo 113-8519, Japan. E-mail: tak-yokota.nuro@tmd.ac.jp

Machado–Joseph disease (MJD) is an autosomal dominant neurodegenerative disorder that is characterized clinically by cerebellar ataxia, pyramidal and extrapyramidal signs, peripheral neuropathy, and ophthalmoplegia. The number of CAG in MJD1 gene repeats is between 13 and 36, whereas in patients this range is expanded from 62 to 84.[1] The pathogenosis of MJD is considered to be caused by "gain of toxic function" of mutant MJD protein.[2,3] Therefore, a most effective and simple gene therapeutic approach for MJD requires the reduction of the aberrant mutant protein. Furthermore, it might be needed to reduce mutant ataxin-3 selectively, leaving wild-type protein intact, because the wild-type MJD1 gene product ataxin-3 should have an important role in cell survival, such as quality control of endoplasmic reticulum[4] and DNA repair.[5]

RNA interference (RNAi) is the process of sequence-specific, posttranscriptional gene silencing, initiated by double-stranded RNA (dsRNA). This has a multistep process that involves the generation of 21 to 23-nucleotide small interfering RNA (siRNA), resulting in degradation of the homologous RNA. The siRNA is long enough to mediate gene-specific suppression but short enough to evade adverse effects of long dsRNA in mammalian cells[6] and is expected to be a powerful tool for gene therapy of human diseases.

We found that the CAG repeat tract in the MJD1 gene is followed by C or G and there is extreme bias of this C/G polymorphism between mutant and normal MJD1 alleles; mutant alleles have exclusively the (CAG)nC, whereas normal alleles have both (CAG)nG and (CAG)nC in a similar frequency[7,8] (Fig 1). Here, we engineered siRNAs to cleave selectively mutant MJD RNA targeting the sequence including this C/G polymorphism.

Materials and Methods

Plasmid Constructs and Small Interfering RNA Design

The expression plasmids of ataxin-3 were kindly given by Dr Akira Kakizuka.[4] The MJD1 cDNA in the plasmid was a truncated fragment including either 22 (normal, pCMX HA-Q22C) or 79 (expanded, pCMX HA-Q79C) repeats of CAG, and was hemagglutinin (HA)-fused on the N terminus. Cytosine after CAG repeat in pCMX HA-Q22C was changed to guanine (pCMX HA-Q22G) using the QuikChange site-directed mutagenesis system (Stratagene, La Jolla, CA). Furthermore, these MJD cDNAs also were subcloned into pIRES-hrGFP-1a (pGFP-Q22G, pGFP-Q22C and pGFP-Q79C; Stratagene).

Four different siRNAs were designed to target the mutant MJD RNA at the junction of CAG repeat and 3′ terminal region (see Fig 1B). A single nucleotide alternation at C/G polymorphism was placed in siRNA at 5th, 8th, 11th, or 14th position from the 5′ end of the sense strand.

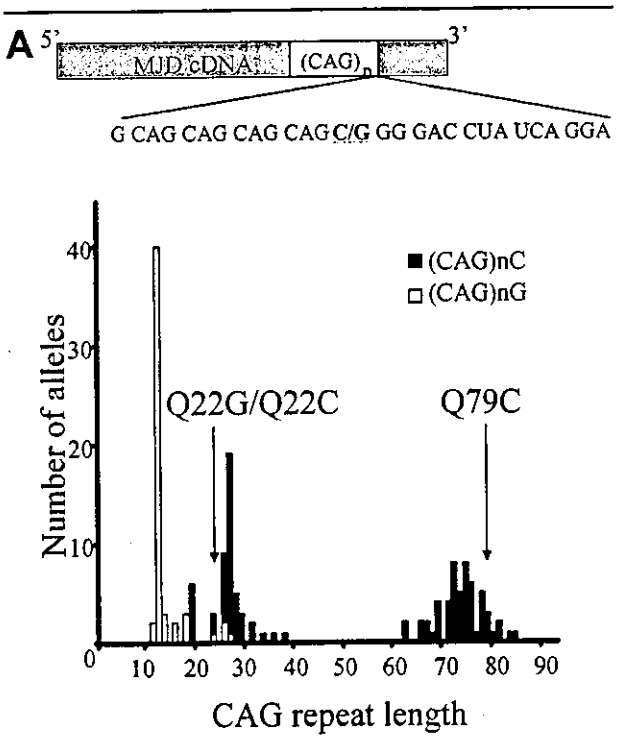

B

Name	Sequence
siRNA MJD1	5'- g cag cgg gac cua uca gga TT-3' 3'-TT c gac gcc cug gau agu ccu -5'
siRNA MJD2	5'- g cag cag cgg gac cua uca TT-3' 3'-TT c gac gac gcc cug gau agu -5'
siRNA MJD3	5'- g cag cag cag cgg gac cua TT-3' 3'-TT c gac gac gac gcc cug gau -5'
siRNA MJD4	5'- g cag cag cag cag cgg gac TT-3' 3'-TT c gac gac gac gac gcc cug -5'
Control (siRNA MJD3-shuffle)	5'- g gag agc aac gcg acc cguTT-3' 3'-TT c cuc ucg uug cgc ugg gca -5'

Fig 1. Design of small interfering RNA (siRNA) sequences targeting the C/G polymorphism in the Machado–Joseph disease (MJD)–1 gene (A) Schema of human MJD1 gene showing C/G polymorphism just downstream from CAG repeat (top panel). The distribution of C/G polymorphism and the CAG repeat length in 56 Japanese MJD patients (bottom panel). All expanded alleles have (CAG)nC, whereas the normal alleles have (CAG)nC and (CAG)nG in similar frequencies (0.46 and 0.54). Arrows indicate the CAG repeat numbers of ataxin-3 expression vector constructs used in this study as wild type and mutant. (B) Sequences of siRNAs used to target (CAG)nC in MJD1 mRNA. Bold characters indicate the site of C/G polymorphism. Uppercase letters indicate deoxyribonucleotides.

Transfections and Western Blotting

To see the effect of siRNAs for MJD RNA on the expression of ataxin-3, we cotransfected both siRNA and ataxin-3-expression plasmids to human embryonic kidney cell line

293T cells (293T) cells. siRNAs were annealed and transfected according to our previously reported method.[9] Four-microgram expression vectors and 10 or 25nM siRNA were cotransfected to 293T cells in six-well culture plates by Lipofectamine Plus reagent (Life Technologies, Rockville, MD).

Twenty-four hours after transfection, cells were harvested by TNG buffer (50mM Tris-HCl, 150mM NaCl, 1% Triton X-100) with protease inhibitor cocktail (Roche, Mannheim, Germany), separated on 15% sodium dodecyl sulfate polyacrylamide gels, and transfered onto polyvinylidene difluoride membrane (Bio-Rad, Richmond, CA). Rat monoclonal anti–HA antibody (Roche) was reacted and detected using an enhanced chemiluminescence detection kit (Amerham Pharmacia Biotech, Arlington Heights, IL).

Assessment of Cell Death

To assess the effect of siRNA on the cell death caused by expression of mutant ataxin-3, we cotransfected Neuro2a cells in 24-well culture plates with pCMX-Q79C (1μg/well) and siRNA (100nM/well). At 48 hours after transfection, the cell death of Neuro2a cells was determined by assaying with both trypan blue exclusion method and measurement of cytoplasmic lactate dehydrogenase (LDH) activity with the Cytotox 96 nonradioactive cytotoxicity assay (Promega, Madison, WI).

Statistical analysis were performed using the Student's *t* test and single-factor analysis of variance followed by Fisher's protected least-significant difference post hoc test.

Results

The mutant ataxin-3, Q79C, was most effectively suppressed by 25nM siRNA MJD3 and was decreased by 96.0% on signal intensity of Western blotting compared with that in control (Fig 2A). In contrast, the expression of the wild-type ataxin-3 Q22G was moderately suppressed by siRNA MJD4, but not clearly influenced by siRNA MJD1, -2, or -3. Therefore, siRNA MJD3 best recognized one nucleotide alternation between C and G and suppressed specifically expression of Q79C, with almost no effect on that of Q22G. Effect of siRNA MJD3 on Q79C expression was dose dependent, but suppression of Q22G was similar at 10 and 25nM concentrations of siRNA (see Fig 2B).

Unexpectedly, siRNA MJD3 did not significantly decrease (22.5%) the expression of another wild-type allele, Q22C, although the target sequence in (CAG)79C and (CAG)22C were the same (see Fig 2B). These suppression effects were confirmed by the reduction in fluorescence of GFP which was bicistronically expressed by internal ribosomal entry site (IRES) with ataxin-3 (pGFP-Q22C or pGFP-Q79C) using DsRed fluorescence as a control for transfection efficiency (see Fig 2C).

Next, by applying siRNA MJD3, we attempted to decrease the cell toxicity induced by mutant ataxin-3. Forty-eight hours after transfection, expression of the mutant MJD (Q79C) was toxic to Neuro2a cells, but those of the wild-type ataxin-3 (Q22G and Q22C) did not influence cell survival. siRNA MJD3 could markedly suppress the toxicity of mutant ataxin-3, decreasing cell death by 62.8% in LDH assay and by 75.9% in trypan blue exclusion method (Fig 3).

Discussion

This is the report of the siRNA which can discriminate mutant and wild-type type RNAs of MJD1 gene: the siRNA MJD3 is highly effective for suppressing mutant ataxin-3, Q79C, with a negligible effect on one wild-type ataxin-3, Q22G, observed in half of Japanese MJD patients, and with much less effect on the other wild-type allele, Q22C, in another half patients. The siRNA has been reported to suppress expression of the mutant androgen receptor RNA including expanded CAG repeat and rescue polyglutamine-mediated cytotoxicity, but it cleaved wild-type RNA with normal CAG repeat in a similar way.[10] During preparation of this article, Miller and his colleagues[11] reported the effective siRNA targeting the C/G polymorphism in MJD1 gene, which suppressed the Q166C expression with only modest effect on Q28G expression, but they did not examine another wild-type allele Q28C.

Diversing effects of mismatch between siRNA and target sequences have been reported. The central single mutation, mismatch in siRNA at 10th and 11th position, produces marked decrease of cleavage siRNA activity.[13] The mismatch in the 5′end has negligible effect on siRNA cleavage activity compared with more centrally located mutation. This bias might be linked to the proposed existence of a "ruler" region in the

Fig 2. Specific effect of the small interfering RNA (siRNA) on the expression of mutant MJD1. (A) Selection of best siRNA to discriminate C/G polymorphism. Western blot analysis of best siRNA for targeting mutant ataxin-3 among siRNA MJD1-4. 293T cells were cotransfected with ataxin-3 expression plasmids (pCMX HA-Q79C and pCMX HA-Q22G) and siRNAs. Tubulin loading controls also are shown. Right panel indicates quantitation of signal intensities. Each percentage suppression was determined by the band intensity with transfection of siRNA MJD3 shuffle as a control. siRNA MJD3 suppressed most Q79C expression, and siRNA MJD1-3 did not influence the Q22G expression. Values are the mean and SEM. (B) Comparison of the effect of siRNA MJD3 on Q79C, Q22G, and Q22C expression. Western blot analysis of the effect of siRNA MJD3 at 10 and 25nM on Q79C, Q22G, and Q22C expression. The results of siRNA(−) were made with siRNA MJD3 shuffle. Right panel indicates quantitation of signal intensities. Almost no suppression on Q22G expression (5.9%) and mild suppression on Q22C expression (22.5%) were noted by siRNA MJD3 at 25nM siRNA in contrast with robust suppression on Q79C expression (96.0%). Bottom panel shows the GFP images of 293T cells cotransfected with pGFP-Q79C/pGFP-Q22C/pGFP-Q22G and siRNA MJD3. pDsRed also was transfected as a control of transfection efficiency (×200).

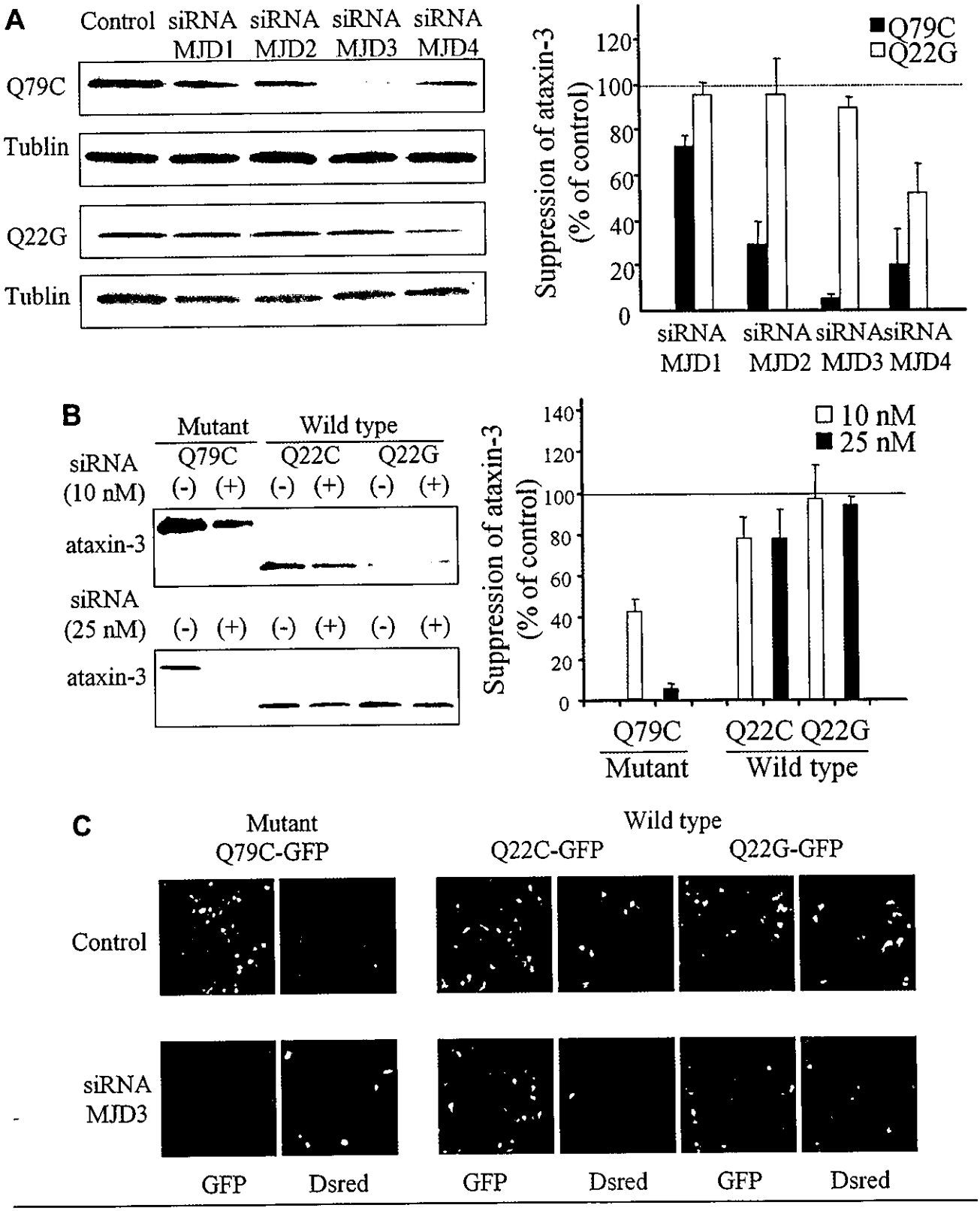
A
Control
siRNA MJD1
siRNA MJD2
siRNA MJD3
siRNA MJD4
Q79C
Tublin
Q22G
Tublin
Suppression of ataxin-3 (% of control)
120
100
80
60
40
20
0
Q79C
Q22G
siRNA MJD1
siRNA MJD2
siRNA MJD3
siRNA MJD4
B
Mutant
Wild type
siRNA (10 nM)
Q79C
Q22C
Q22G
(-) (+) (-) (+) (-) (+)
ataxin-3
siRNA (25 nM)
(-) (+) (-) (+) (-) (+)
ataxin-3
Suppression of ataxin-3 (% of control)
140
120
100
80
60
40
20
0
10 nM
25 nM
Q79C
Q22C Q22G
Mutant
Wild type
C
Mutant
Q79C-GFP
Wild type
Q22C-GFP
Q22G-GFP
Control
siRNA MJD3
GFP
Dsred
GFP
Dsred
GFP
Dsred

Figure 2

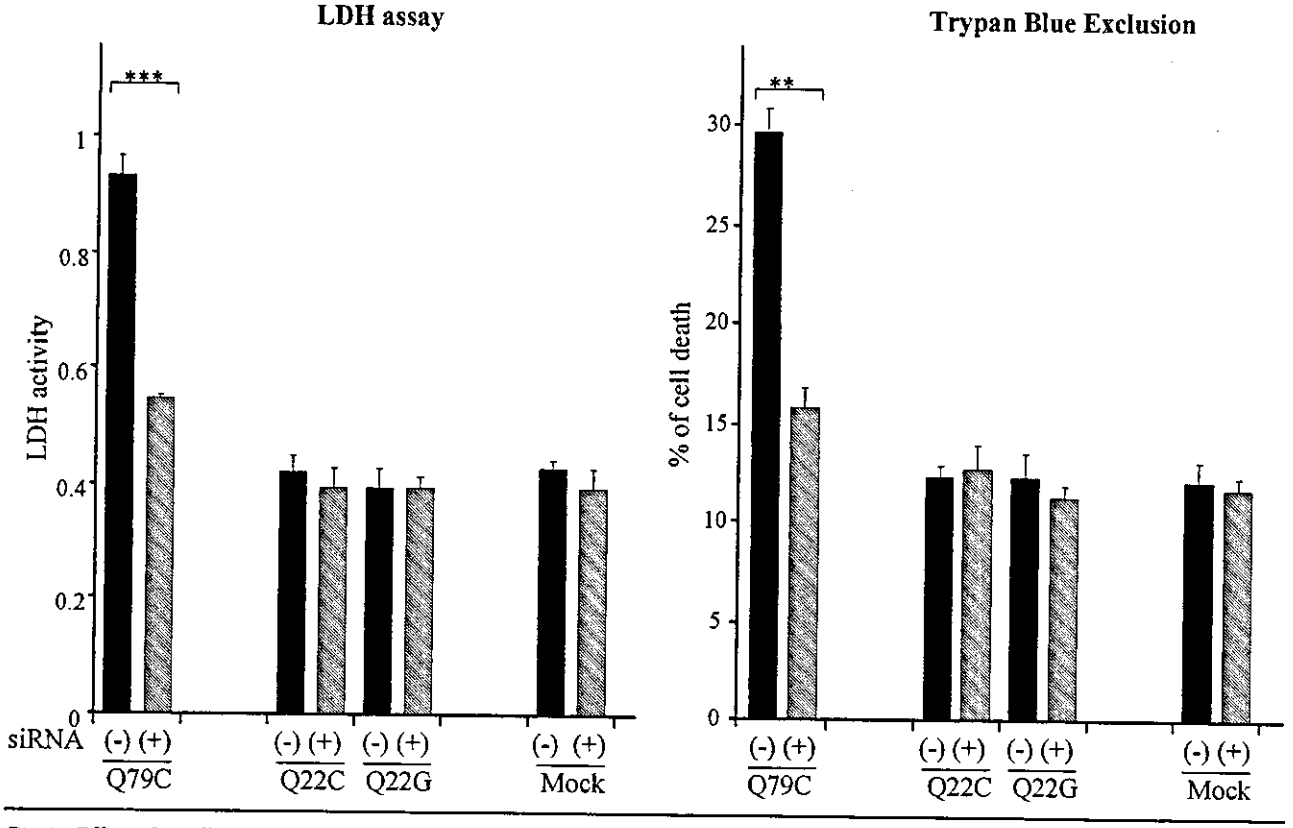

*Fig 3. Effect of small interfering RNA (siRNA) MJD3 on the mutant ataxin-3–induced toxicity in mammalian cells. siRNA MJD3 rescues the cell death induced by overexpression of Q79C, Q22C, and Q22G on lactate dehydrogenase (LDH) assay and trypan blue exclusion method (***$p < 0.0001$, **$p < 0.01$). Overexpression of Q22G or Q22C did not show toxicity. pcDNA3.1 plasmid (Invitrogen, La Jolla, CA) was used as mock. Values are the mean and SEM. The result of siRNA(−) was made with siRNA MJD3 shuffle.*

siRNA that is used by the RNA-induced silencing complex (RISC) complex to "measure" the target RNA for cleavage .[13] In four siRNAs examined in our study, siRNAs (siRNA MJD2 and -3) with central mismatch have better discrimination than that with outside mismatch (siRNA MJD1 and -4), and this result is consistent with the previously reported results.

Surprisingly, there was much difference between the effect of siRNA on Q22C and Q79C, although their target sequences of siRNAs were the same. This is the first report to our knowledge of sequence-independent discrimination of mutant and wild-type alleles by siRNA. One possible reason for this difference is that not all RNA sequences are equally accessible to siRNAs: some sequences might be buried within the secondary structure of target RNAs especially when they are highly folded.[15] We also experienced that the best target site of siRNA for the highly folded RNA was almost same as that for ribozyme, which cleavage efficiency is much influenced by the secondary structure of target RNA.[9] The target site of C/G polymorphism is just downstream from the CAG repeat, which represents a tight stem form in their secondary structure on a computer prediction. Although we have no data indicating that siRNA MJD3 is more accessible to (CAG)79C than (CAG)22C, a change of secondary structure of the MJD RNA due to a large difference of the CAG repeat length might affect the efficiency of siRNA MJD3. Another possible explanation is that there is a RNA-binding protein preferentially binding (CAG)22C over (CAG)79C, which interferes the access of siRNA MJD3 to (CAG)22C RNA. The RNA-binding protein to MJD RNA has not been found, but CUG repeat in myotonic dystrophy protein kinase (DMPK) RNA binds the proteins including CUG-binding protein in repeat length-dependent manner.[15] Moreover, existence of a RNA-binding protein attaching CAG repeat was suggested in Huntington's disease.[16] Further studies are needed to make clear the mechanism for the difference of the siRNA effect on (CAG)79C and (CAG)22C.

We are in the process of making adeno-associated virus and transgenic mice expressing siRNA MJD3 to investigate the efficacy of siRNAs in vivo. Although a less invasive delivery method for introducing siRNAs into a larger area of cerebellum would be needed for clinical feasibility, the efficiency of our siRNA to specifically reduce the expression and toxicity of mutant

ataxin-3 in cells suggests that this mRNA-targeting approach by siRNA might provide effective therapy for MJD.

This work was supported by grants from the Ministry of Education, Science and Culture of Japan (14570582; T.Y.) and from the Ministry of Health, Labor and Welfare of Japan (H14-KOKORO-018; T.Y.), and 21st Century Center of Excellence (COE) Program Fellowship (L.Y.).

We thank Dr A. Kakizuka for providing expression vectors of MJD gene.

References

1. Kawaguchi Y, Okamoto T, Taniwaki M, et al. CAG expansions in a novel gene for Machado-Joseph disease at chromosome 14q32.1. Nat Genet 1994;8:221–228.
2. Ross CA. When more is less: pathogenesis of glutamine repeat neurodegenerative diseases. Neuron 1995;15:493–496.
3. Ikeda H, Yamaguchi M, Satoshi S, et al. Expanded polyglutamine in the Machado-Joseph disease protein induced cell death in vitro and in vivo. Nat Genet 1996;13:196–202.
4. Kobayashi T, Tanaka K, Inoue K, Kakizuka A. Functional ATPase activity of p97/valosin-containing protein (VCP) is required for the quality control of endoplasmic reticulum in neuronally differentiated mammalian PC12 cells. J Biol Chem 2002;277:47358–47365.
5. Wang G, Sawai N, Kotliarova S, et al. Ataxin-3, the MJD1 gene product, interacts with the two human homologs of yeast DNA repair protein RAD23, HHR23A and HHR23B. Hum Mol Genet 2000;9:1795–1803.
6. Elbashir S, Harborth J, Lendeckel W, et al. Duplexes of 21 nucleotide RNAs mediate RNA interference in cultured mammalian cells. Nature 2001;411:494–498.
7. Matsumura R, Takayanagi T, Murata K, et al. Relationship of (CAG)nC configuration to repeat instability of the Machado-Joseph disease gene. Hum Genet 1996;98:643–645.
8. Gaspar C, Lopes-Cendes I, Hayes S, et al. Ancestral origins of the Machado-Joseph disease mutation: a worldwide haplotype study. Am J Hum Genet 2001;68:523–528.
9. Yokota T, Sakamoto N, Enomoto Y, et al. Inhibition of intracellular hepatitis C virus replication by synthetic and vector-derived small interfering RNAs. EMBO Rep 2003;4:602–608.
10. Caplen NJ, Taylor JP, Statham VS, et al. Rescue of polyglutamine-mediated cytotoxicity by double-stranded RNA-mediated RNA interference. Hum Mol Genet 2002;11:175–184.
11. Miller VM, Xia H, Marrs GL, et al. Allele-specific silencing of dominant disease genes. Proc Natl Acad Sci USA 2003;100:7195–7200.
12. Elbashir SM, Martinez J, Patkaniowska A, et al. Functional anatomy of siRNAs for mediating efficient RNAi in *Drosophila melanogaster* embryo lysate. EMBO J 2001;20:6877–6888.
13. Holen T, Amarzguioui M, Wiiger MT, et al. Positional effects of short interfering RNAs targeting the human coagulation trigger tissue factor. Nucleic Acids Res 2002;30:1757–1766.
14. Yoshinari K, Miyagishi M, Taira K, et al. Effect on RNAi of the tight structure, sequence and position of the targeted region. Nucleic Acids Res 2004;32:691–699.
15. Philips AV, Timchenko L, Cooper TA. Disruption of splicing regulated by a CUG-binding protein in myotonic dystrophy. Science 1998;280:737–741.
16. McLaughlin BA, Spencer C, Eberwine J. CAG trinucleotide RNA repeats interact with RNA-binding proteins. Am J Hum Genet 1996;59:561–569.

Published by Wiley-Liss, Inc., through Wiley Subscription Services

MOLECULAR AND CELLULAR BIOLOGY, July 2004, p. 6298–6310
0270-7306/04/$08.00+0 DOI: 10.1128/MCB.24.14.6298–6310.2004

Vol. 24, No. 14

Interferon Regulatory Factor 1 (IRF-1) and IRF-2 Distinctively Up-Regulate Gene Expression and Production of Interleukin-7 in Human Intestinal Epithelial Cells

Shigeru Oshima,[1]† Tetsuya Nakamura,[1]† Shin Namiki,[1] Eriko Okada,[1] Kiichiro Tsuchiya,[1] Ryuichi Okamoto,[1] Motomi Yamazaki,[1] Takanori Yokota,[2] Masatoshi Aida,[3] Yuki Yamaguchi,[3] Takanori Kanai,[1] Hiroshi Handa,[3] and Mamoru Watanabe[1]*

Department of Gastroenterology and Hepatology[1] and Department of Neurology and Neurological Sciences,[2] Graduate School, Tokyo Medical and Dental University, Bunkyo-ku, Tokyo 113-8519, and Graduate School of Bioscience and Biotechnology, Tokyo Institute of Technology, Yokohama 226-8501,[3] Japan

Received 10 September 2003/Returned for modification 16 January 2004/Accepted 19 April 2004

Intestinal epithelial cell-derived interleukin (IL)-7 functions as a pleiotropic and nonredundant cytokine in the human intestinal mucosa; however, the molecular basis of its production has remained totally unknown. We here showed that human intestinal epithelial cells both constitutively and when induced by gamma interferon (IFN-γ) produced IL-7, while several other factors we tested had no effect. Transcriptional regulation via an IFN regulatory factor element (IRF-E) on the 5′ flanking region, which lacks canonical core promoter sequences, was pivotal for both modes of IL-7 expression. IRF-1 and IRF-2, the latter of which is generally known as a transcriptional repressor, were shown to interact with IRF-E and transactivate IL-7 gene expression in an IFN-γ-inducible and constitutive manner, respectively. Indeed, tetracycline-inducible expression experiments revealed that both of these IRF proteins up-regulated IL-7 protein production, and their exclusive roles were further confirmed by small interfering RNA-mediated gene silencing systems. Moreover, these IRFs displayed distinct properties concerning the profile of IL-7 transcripts upon activation and expression patterns within human colonic epithelial tissues. These results suggest that the functional interplay between IRF-1 and IRF-2 serves as an elaborate and cooperative mechanism for timely as well as continuous regulation of IL-7 production that is essential for local immune regulation within human intestinal mucosa.

Intestinal epithelial cells (IECs) function as active participants in local immune regulation via the secretion of a variety of cytokines. Among these, interleukin-7 (IL-7) is particularly important in terms of its pleiotropic functions in the intestinal immune system. Studies have demonstrated that IEC-derived IL-7 stimulates the proliferation of lamina propria lymphocytes and intraepithelial lymphocytes (IELs) (5, 30) and also enhances cytokine release from lamina propria lymphocytes in humans (20). In addition, analyses in mice have revealed the nonredundant functions of IL-7, because inactivation of IL-7 or the IL-7 receptor gene resulted in severely impaired development of γδ-IELs, Peyer's patches, and cryptopatches, all of which play critical roles in mucosal immune regulation (13, 21, 29). These findings suggest that IL-7 production from IECs might be tightly controlled for variable levels of production that properly respond to the altered status of mucosal lymphocytes and also for the constitutive levels of secretion that might support the nonredundant functions of IL-7, for example, on the development of gut-associated lymphoid tissues. Previously, our group has demonstrated that the mRNA and protein of IL-7 are expressed throughout the epithelial layer of human colonic tissues, and the epithelial goblet cells are the type of cells where the expression of IL-7 is relatively abundant (30). To date, however, the mechanisms of IL-7 production in human IECs are poorly defined.

Lack of knowledge about the mechanism of IL-7 production is not confined to IECs but is also the case with other tissue-derived cells of human origin. Previous reports demonstrated that IL-7 production from human bone marrow (BM) stromal cells, the major cell type from which IL-7 is produced in vivo, was regulated by several cytokines such as IL-1, tumor necrosis factor alpha (TNF-α) and transforming growth factor beta (TGF-β) (27, 34); however, the intracellular mechanisms of these regulations have remained unclear. In addition, little is known about the mechanisms by which IL-7 is constitutively produced, while such cells as BM stromal cells exhibited the ability to produce a substantial amount of IL-7 even in the absence of specific cytokines in vitro (27, 34). Moreover, studies on murine tissue-derived cells rather complicated the question as to the mechanisms of IL-7 production in human cells, since these studies implied a different mechanism for murine IL-7 gene expression (3), despite a high degree of conservation in the 5′ flanking region of the IL-7 genes of both species (3, 8, 23). For example, in murine keratinocytes Pam 212 cells, ex-

* Corresponding author. Mailing address: Department of Gastroenterology and Hepatology, Graduate School, Tokyo Medical and Dental University, 1-5-45 Yushima, Bunkyo-ku, Tokyo 113-8519, Japan. Phone: 81 3 5803 5973. Fax: 81 3 5803 0262. E-mail: mamoru.gast@tmd.ac.jp.

† S.O. and T.N. contributed equally to this work.

pression of the IL-7 gene was not influenced by IL-1, TNF-α, or TGF-β but was up-regulated by another cytokine, gamma interferon (IFN-γ) (3), indicating that murine cells respond differently than human BM stromal cells to these cytokines (27, 34). These collective findings suggest that IL-7 production might be under the control of a tissue-specific and/or a species-specific regulatory mechanism. Therefore, it seems crucial to clarify the mechanisms of IL-7 production in human IECs to gain a better understanding of the functions of this cytokine on local immune regulation.

In this study, using human colonic epithelial cell lines, we showed that IL-7 protein was produced both constitutively and in response to IFN-γ in human IECs. The transcriptional regulation via an interferon regulatory factor element (IRF-E) was important for IL-7 production in human IECs, which is consistent with the previous report on murine keratinocytes. Of note, it was found that not only IRF-1 but also IRF-2, generally known as a transcriptional repressor, up-regulated IL-7 production. Intriguingly, IRF-1 and IRF-2 exclusively exerted their functions in an IFN-γ-inducible and constitutive manner, respectively, with properties to induce different sets of IL-7 transcript upon activation. Along with the demonstration that both IRF-1 and IRF-2 were expressed in normal human colonic epithelial cells, these data suggest that the functional interplay between IRF-1 and IRF-2 might serve as an elaborate mechanism for the finely tuned regulation of IL-7 production that is indispensable for local immune regulation within the human intestinal mucosa.

MATERIALS AND METHODS

Cell culture. Human colon carcinoma-derived DLD-1 and HT29-18N2 cells were maintained in Dulbecco's modified Eagle medium supplemented with 10% fetal bovine serum and 1% penicillin-streptomycin. Except where indicated otherwise, cells were seeded at a density of 3×10^5 cells/ml in the medium 36 h prior to each experiment.

ELISA. Cells at a density of 8×10^5 cells per ml of culture medium were seeded onto 24-well plates. After 36 h of culture, the medium was removed, and the cells were washed twice with phosphate-buffered saline. Following the addition of 1 ml of culture medium alone, or medium containing either human IL-1β, TNF-α, TGF-β, IFN-γ (PeproTec), or doxycycline (DOX; Clontech), cells were cultured for 24 h, and human IL-7 protein levels in the culture supernatants were measured by a human IL-7 enzyme-linked immunosorbent assay (ELISA) kit (R&D Systems).

Semiquantitative reverse transcription (RT)-PCR. Total RNA was isolated by using Trizol reagent (Invitrogen) according to the manufacturer's instructions. Aliquots of 5 μg of total RNA were used for cDNA synthesis in 21 μl of reaction volume. One microliter of cDNA was amplified with 0.25 U of LA *Taq* polymerase (TaKaRa) in a 25-μl reaction. Sense (S) and antisense (AS) primers used here were as follows: S1, 5′-AGCTTGCTCCTGCTCCAGTT-3′; S2, 5′-GAGATCATCTGGGAAGTCTTTTACC-3′; S3, 5′-ACTTGTGGCTTCCGTGCACACATTA-3′; AS1, 5′-TGCATTTCTCAAATGCCCTAATCCG-3′; and AS2, 5′-ATCCGCCAGCAGTGTACTTTCAGTT-3′ for human IL-7 (see Fig. 2A). For glyceraldehyde 3-phosphate dehydrogenase (G3PDH) amplification, the primers were5′-TGAAGGTCGGAGTCAACGGATTTGGT-3′ (S) and and 5′-CATGTGGGCCATGAGGTCCACCAC-3′ (AS). Each cycle of PCR amplification consisted of denaturation at 94°C for 30 sec, annealing at 61°C for 30 sec, and extension at 72°C for 30 sec. Twenty-seven cycles were performed for IL-7, and 17 cycles were performed for G3PDH, and the amplification for each gene was in the linear curve under these conditions. PCR products were separated on 1.5% agarose gels, stained by ethidium bromide, and visualized by using a Lumi-Imager F1 system (Roche).

Northern blotting. Poly(A)$^+$ mRNA was isolated by using a FastTrack 2.0 kit (Invitrogen) according to the manufacturer's instructions. Northern blotting was performed as described previously (22) by using 15 μg of poly(A)$^+$ mRNA. The cDNA probe corresponding to nucleotides at positions −55 to +681 (coding sequence [CS] probe) and −539 to −242 (5′ untranslated region [UTR] probe) for human IL-7 were generated by RT-PCR by using the primers S1/AS1 and S3/AS2, respectively, from an RNA sample of DLD-1 cells as described above. The probe for G3PDH was also generated by RT-PCR by using the primers described above. Hybridization was carried out at 42°C overnight for IL-7 and at 55°C for 2 h for G3PDH.

RLM-RACE. Determination of the transcription initiation sites of the human IL-7 gene was accomplished by RNA ligase-mediated [RLM] 5′ rapid amplification of cDNA ends [RACE] by using a GeneRacer Kit (Invitrogen). In brief, poly(A)$^+$ mRNAs extracted from IFN-γ-stimulated (6 h) DLD-1 cells were treated with calf intestinal phosphatase to eliminate 5′ phosphates from truncated mRNA without affecting 5′ capped intact mRNA. The dephosphorylated RNA was then treated with tobacco acid pyrophosphatases to remove the 5′ cap structure. The GeneRacer RNA Oligo was ligated to the 5′ end of the decapped mRNA by using T4 RNA ligase. First-strand cDNA synthesis was performed by reverse-transcribing the ligated mRNA in the presence of the GeneRacer oligo dT primer. Sequential PCRs were performed by using a primer set of the GeneRacer 5′ primer and 3′ reverse IL-7 gene-specific primer 1 (GSP-1) and then by using the nested primer set of the GeneRacer 5′ nested primer and 3′ reverse IL-7 GSP-2 to amplify only the cDNAs that have the GeneRacer RNA Oligo ligated to the 5′ end. As a control, PCR with a primer set for amplifying the 5′ part of the human β-actin gene was also performed in parallel, according to the manufacturer's recommendation. The primers used were 5′-TGCCCTAATCCGTTTTGACCATGGTG-3′ (IL-7 GSP-1) and 5′-GCAACAGAACAAGGATCAGGGGAGG-3′ (IL-7 GSP-2). PCR products of around 600 and 300 bp were gel purified and cloned into the pGEM-T vector (Promega) independently, and then 10 clones of each were sequenced. All the clones contained the IL-7 gene sequence along with the adapter sequences, indicating these clones to be derived from mRNAs retaining complete 5′ ends.

Plasmids. The human IL-7 DNA fragment between either position −3194, −1322, −609, or −282 and −3 was amplified from human genomic DNA by PCR and ligated into the pGL3 Basic luciferase reporter plasmid (Promega) to create −3194-Luc, −1322-Luc, −609-Luc, and −282-Luc. The nucleotide position number was assigned relative to the translation start site (+1). A series of 5′ deletions of the −609-Luc, shown as −362-Luc, −251-Luc, and −215-Luc, was constructed by unidirectional digestion by using an exonuclease III. An internal deletion mutant −609-Luc-Δ-282/-251 was constructed by PCR-mediated mutagenesis. Plasmids −609-mtIRF-E-Luc and −282-mtIRF-E-Luc, both of which contain a 4-bp mutation within IRF-E, were also constructed by PCR-mediated mutagenesis. Introduced mutations and the wild-type sequences within the region of positions −280 to −253 were given with top strand sequences as follows: mutant, 5′-AAGCGCAAAGTAGAGGCTGAGGGTACAC-3′ (underlined residues indicate introduced mutations); wild type, 5′-AAGCGCAAAGTAGAAACTGAAAGTACAC-3′. Expression vectors pcDNA3-IRF-1 and pcDNA3-IRF-2 were prepared by subcloning the PCR-amplified open reading frame of human IRF-1 and IRF-2 cDNA into a pcDNA3 (Invitrogen). To construct tetracycline (TET)-inducible expression plasmids, the open reading frames of IRF-1 and IRF-2 were subcloned into a pcDNA4/TO/Myc/His (Invitrogen) in frame. All constructs were verified by DNA sequencing.

Transient transfection and reporter assays. DLD-1 cells seeded in a 60-mm culture dish were transfected with 3 μg of reporter plasmid along with 10 ng of pRL-tk plasmid (Promega) as described previously (22). Cells were harvested 24 h after transfection, lysed by three cycles of freezing and thawing, and then luciferase activities were measured by a luminometer (Turner Designs). Luciferase activities as indicated by arbitrary unit were normalized by renilla luciferase activities in each sample.

EMSA. The preparation of nuclear extracts and electrophoretic mobility shift assays (EMSA) were performed essentially as described previously (22), except for the use of 0.5 μg of poly(dI-dC) · poly(dI-dC) per binding reaction. A DNA probe and its mutated version were prepared by annealing oligonucleotides as follows: top strand, 5′-AAGCGCAAAGTAGAAACTGAAAGT-3′, and bottom strand, 5′-GTGTACTTTCAGTTTCTACTTTG-3′, for the wild-type probe; and top strand, 5′-AAGCGCAAAGTAGAGGCTGAGGGT-3′, bottom strand, 5′-GTGTACCCTCAGCCTCTACTTTG-3′, for the mutant probe. For competition experiments, a 20-fold excess of unlabeled double-stranded probe or its mutated version was added prior to the labeled probe. In supershift experiments, antibodies (Santa Cruz Biotechnology) against either IRF-1 (catalogue no. sc-497), IRF-2 (sc-498), IRF-3 (sc-9082), IRF-4 (sc-6059), IRF-7 (sc-9083), IRF-8 (sc-6058), or IRF-9 (sc-496) were used.

Immunoblotting. Immunoblotting was performed as described elsewhere (22). Twenty-five micrograms of nuclear extracts was analyzed by using anti-IRF-1 (catalogue no. sc-497), anti-IRF-2 (sc-498), and anti-upstream factor (USF)-2 (sc-861) antibodies (all from Santa Cruz Biotechnology) at a 1:500 dilution as a

primary antibody. Proteins were visualized with an enhanced chemiluminescence detection system (Amersham Bioscience).

Establishing tetracycline-regulated IRF-1- and IRF-2-expressing DLD-1 cell lines. Sublines of DLD-1 cells, in which the expression of either IRF-1 or IRF-2 is inducible under the control of the addition of TET, were established by using a T-REx System (Invitrogen). In brief, a DLD-1-derived subclone that constitutively expresses the TET repressor (TR) was created by transfecting parental DLD-1 cells with a plasmid pcDNA6/TR (Invitrogen). Several clones were selected in the culture medium containing blasticidin (7.5 μg/ml; Invitrogen). An appropriate clone was isolated, designated as DLD-1/TR cells, and then transfected with either expression plasmid pcDNA4/TO/IRF-1-Myc/His or pcDNA4/TO/IRF-2-Myc/His. Cells stably expressing each of these genes were selected in the presence of 750 μg of Zeocin (Invitrogen) per ml to establish the sublines designated as DLD-1/TR/IRF-1-tag or DLD-1/TR/IRF-2-tag cells. In all experiments, we used DOX as an alternative inducer of gene expression because it has a longer half-life than TET.

siRNA experiments. All small interfering RNA (siRNA) duplex oligonucleotides were synthesized and subsequently annealed for use. DLD-1 cells were seeded at a density of 3×10^5 cells per ml onto a 24-well plate or a 100-mm culture dish. After 36 h, cells were transfected with 100 nM siRNA oligonucleotides as described previously (37), and the siRNA-containing medium was removed after 12 h of transfection. Cells were cultured for an additional 12 h under the usual conditions, and then the medium was exchanged with either the medium alone or medium containing IFN-γ. For immunoblotting analysis, cells were collected from the 100-mm dishes after 12 h of medium exchange, and the nuclear extracts were isolated. For the ELISA, the culture supernatants were collected from the 24-well plates after 24 h of medium exchange. The sequences of siRNAs used here were as follows (S strand only): IRF-1, CCAAGAACCA GAGAAAAGA*TT*; IRF-2, CUCUUUAGAAACUGGGCAA*TT*; and negative control (G85R mutant superoxide dismutase), UGUUGGAGACUUCGGCAA U*TT*. Italicized letters indicate deoxynucleotides.

ChIP assays. A chromatin immunoprecipitation (ChIP) assay was performed essentially as described previously (24) with some modifications. DLD-1 cells seeded onto a 150-mm dish were stimulated with IFN-γ or left untreated for 6 h, cross-linked with 1% formaldehyde for 5 min at room temperature, and then quenched by adding glycine. Cells were washed with phosphate-buffered saline, resuspended in 1 ml of lysis buffer (10 mM Tris-HCl [pH 8.0], 0.25% Triton X-100, 10 mM EDTA, and 0.5 mM EGTA) and left on ice for 10 min. After centrifugation, the nuclei were washed with 1 ml of wash buffer (10 mM Tris-HCl [pH 8.0], 200 mM NaCl, 10 mM EDTA, and 0.5 mM EGTA, 10 mM sodium butyrate, 20 mM β-glycerophosphate, 100 μM sodium orthovanadate, 1 μM microcystin, and the protease inhibitor cocktail) and resuspended in 400 μl of sonication buffer (10 mM Tris-HCl [pH 8.0], 100 mM NaCl, 1 mM EDTA, and 0.5 mM EGTA). The sonication was performed in two steps by using a VP-152 system (TAITEC); the first step was carried out for 5 min, followed by the addition of 50 μl of 10% sodium dodecyl sulfate (SDS) and incubation for 1 h to solubilize the chromatin, and then the second sonication was performed for 4 min. This yielded genomic fragments with an average size of 500 bp. Aliquots (100-μl) of sheared chromatin were diluted into 1 ml of radioimmunoprecipitation assay (RIPA) buffer (10 mM Tris-HCl [pH 8.0], 1% Triton X-100, 0.1% SDS, 0.1% sodium deoxycholate, 1 mM EDTA, 0.5 mM EGTA, and 140 mM NaCl) and precleared with 50 μl of protein G-Sepharose (50% slurry in RIPA buffer) for 1 h at 4°C. Immunoprecipitation was performed overnight at 4°C with 10 μg of an anti-IRF-1 (catalogue no. sc-497), anti-IRF-2 (sc-498), normal mouse immunoglobulin G (IgG; sc-2025) (all from Santa Cruz Biotechnology), or an antihistone H3 antibody (Abcam, Inc.). A 20-μl aliquot of 50% protein G-Sepharose slurry (same as above but containing 2 mg of herring sperm DNA per ml and 2 mg of bovine serum albumin per ml) was added to each and incubated for 1 h at 4°C. Precipitates were washed sequentially in RIPA buffer three times, in 0.5 M NaCl RIPA buffer (same as RIPA buffer but with 500 mM NaCl) three times, in LiCl wash buffer (10 mM Tris-HCl [pH 8.0], 0.25 M LiCl, 1% NP-40, 1% sodium deoxycholate, 1 mM EDTA, 1 mM EGTA, 10 mM sodium butyrate, 100 μM sodium orthovanadate, and the protease inhibitor cocktail) twice, and in TE buffer (10 mM Tris-HCl [pH 8.0], 1 mM EDTA) twice, for 3 min for each wash. Samples were extracted twice with 50 μl of elution buffer (1% SDS, 0.1 M NaHCO3, 10 mM dithiothreitol) and digested with 2 μg of proteinase K at 37°C for 4 h. Then 4 μl of 5 M NaCl was added, and the samples were incubated at 65°C overnight to reverse cross-linking. DNA fragments were recovered by phenol-chloroform extraction and ethanol precipitation.

The genomic DNA fragments in the immunoprecipitated samples were analyzed by PCR by using a primer set for amplifying the −539 to −159 region of the human IL-7 gene (5′-ACTTGTGGCTTCCGTGCACACATTA-3′ and 5′-GACTGCAGTTTCATCCATCCCAAG-3′) to detect the IRF-E-containing fragment, and another set for the +976 to +1337 region (5′-GCTCTTTCTTTT GATGGCTACTCCG-3′ and 5′-TAGCCCATGATTCATATAACTGTGC-3′; numbers indicate the positions on the genomic DNA relative to the translation start site) (see Fig. 8A) as controls. Initially, quantitative PCR on a LightCycler system (Roche) was performed to quantify the immunoprecipitated DNA. A 5-μl aliquot from a total of 100 μl of DNA solution was amplified and the threshold cycle was obtained from each amplification curve. In practice, DNA fragments were nonspecifically and reproducibly recovered after the ChIP assay in the absence of specific antibody but were usually amplified 5 to 6 cycles later than specifically recovered fragments. By using software provided by the manufacturer, the amount of DNA fragment in each sample was calculated relative to the standard curve obtained by the three different dilutions of input DNAs (10, 1, and 0.1%). Three independent chromatin preparations were made, and the average value obtained for each sample was indicated as a percentage of total input DNA. The same amounts of DNA samples or the diluted inputs were also analyzed by conventional PCR in parallel with the following parameters: denaturation at 94°C for 15 s, annealing at 61°C for 30 s, and extension at 72°C for 30 s for 37 cycles. The products were resolved by agarose gel electrophoresis, stained with ethidium bromide, and visualized by using a Lumi-Imager F1 system (Roche).

Immunohistochemistry. Normal colonic mucosae were obtained from three patients with colorectal cancer who underwent colectomy. Written informed consent was obtained from all patients, and these experiments were approved by the Tokyo Medical and Dental University Hospital Committee on Human Subjects. Samples fixed by 4% paraformaldehyde were cut into 8 μm-thick sections, treated with 0.5% hydrogen peroxide in methanol solution, blocked for 45 min, and then incubated with either an anti-IRF-1 (catalogue no. sc-497; Santa Cruz Biotechnology), an anti-IRF-2 (sc-13042), or purified rabbit IgG (10 mg/ml; negative control) overnight at 4°C. The sections were incubated with biotinylated goat antirabbit IgG for 60 min and reacted with streptavidin-enzyme conjugates (Vector Laboratories Inc), and then the peroxidase activities were developed by diaminobenzidin. After the samples were counterstained with hematoxylin, the localization of IRF-1 or IRF-2 was examined by light microscopy.

RESULTS

Human IECs constitutively produce IL-7, and IL-1, TNF-α, and TGF-β have no influence on the levels of IL-7 production, but IFN-γ does. To investigate the mechanisms of IL-7 production in human IECs, human colonic epithelial cell lines, DLD-1 and HT29-18N2 cells, were analyzed. Previous reports showed that both IL-1 and TNF-α had enhancing effects on IL-7 production in human BM stromal cells or osteoblasts (34), while TGF-β had suppressive effects on IL-7 production in BM stromal cells (27). In contrast, shown with murine keratinocytes, none of these cytokines had any effect, while IFN-γ solely exhibited enhancing effects on IL-7 mRNA expression among various factors (3). Therefore, to test whether IL-7 production in human IECs is also diversely regulated by these cytokines, DLD-1 and HT29-18N2 cells were incubated for 24 h with either IL-1, TNF-α, TGF-β, IFN-γ, or the medium alone, and IL-7 production was measured by ELISA. As shown in Fig. 1, both of these cells constitutively produced substantial amounts of IL-7 protein, with a higher concentration per cell number in DLD-1 than in HT29-18N2 cells. In addition, treatment with IFN-γ significantly enhanced IL-7 production in both cell types, while stimulation with IL-1, TNF-α, or TGF-β had no effect (Fig. 1). We also tested the possibility that TGF-β might act as an inhibitory factor not for the constitutive but for the inducible production of IL-7, but treatment with TGF-β did not affect IFN-γ-inducible IL-7 production (Fig. 1). These data indicated that human IECs produce IL-7 both constitutively and in response to IFN-γ, while several other cytokines have no regulatory effect on this process.

Transcription start sites of the human IL-7 gene are clustered within two distinct regions, and IFN-γ preferentially

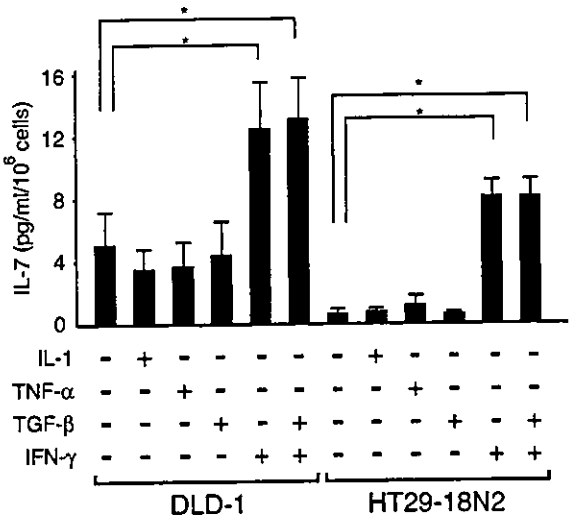

FIG. 1. Human IECs constitutively produce IL-7, and IL-1, TNF-α, and TGF-β do not influence the levels of IL-7 production, whereas IFN-γ does. DLD-1 and HT29-18N2 cells were cultured in medium alone or in medium containing 50 ng of either IL-1, TNF-α, TGF-β, IFN-γ, or IFN-γ plus TGF-β per ml for 24 h. The supernatants were collected and assayed for IL-7 production by ELISA. Results are the means ± standard deviations of three independent experiments. *, $P < 0.05$ by a paired Student t test.

induces short species of mRNA via a selective usage of downstream initiation sites. Human tissues have been shown to express two major IL-7 mRNAs of ~1.8 and ~2.4 kb, and this has been inferred as a result of alternative polyadenylation (8). To examine whether constitutive and IFN-γ-inducible IL-7 protein production is regulated at the mRNA level, we next assessed the expression of IL-7 transcripts by Northern blot analysis by using a cDNA probe covering the IL-7 protein coding sequences (Fig. 2A, CS probe). In DLD-1 cells, two major mRNA species were clearly observed in the absence of IFN-γ (Fig. 2B, left). Since each of these bands migrated somewhat heterogeneously, it was difficult to determine the precise size of these transcripts. However, the analysis of mRNAs extracted from SK-Hep1 cells, human hepatocellular carcinoma cells originally used for the cloning of the human IL-7 gene (8), showed equally migrating bands (data not shown). Thus, we tentatively equated these transcripts with those described previously (8). When DLD-1 cells were treated with IFN-γ, ~1.8-kb mRNA was significantly induced within 6 h, whereas the increase in ~2.4-kb mRNA was modest (Fig. 2B, left). Although the basal level of IL-7 mRNA was lower in HT29-18N2 cells than could be visualized, these cells displayed a similar pattern of IL-7 mRNA expression: IFN-γ significantly induced expression of ~1.8-kb and, to a lesser extent, ~2.4-kb of mRNAs (Fig. 2B, right). These data indicated that the levels of IL-7 protein production correlate well with those of mRNA expression and that IFN-γ treatment predominantly induces the short mRNA species of the IL-7 gene. Interestingly, in murine keratinocytes, IFN-γ treatment was demonstrated to induce the expression of relatively short species of IL-7 mRNA through the use of alternative transcription start sites (3). Given an analogy in IFN-γ-dependent induction of selective IL-7 transcripts between human IECs and murine keratinocytes, it seemed possible that the mechanisms of IFN-γ-dependent IL-7 gene expression are, at least in part, conserved between these two cell types.

To date, a detailed analysis of the transcription start sites for the human IL-7 gene has not been reported. We thus at-

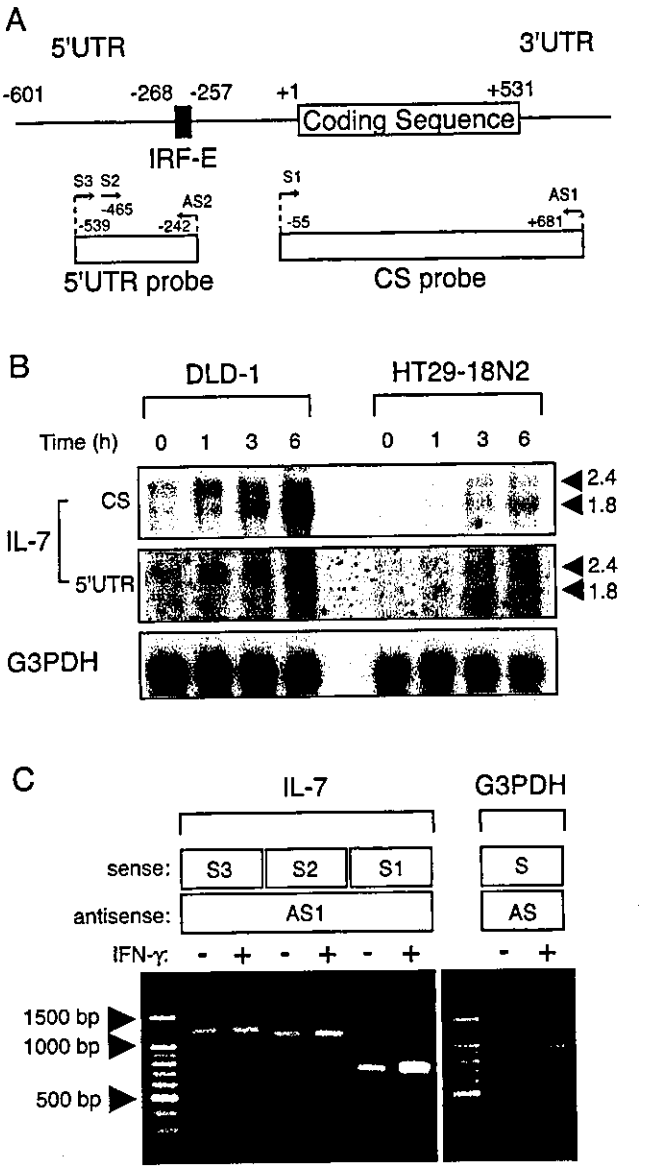

FIG. 2. IFN-γ-dependent and -independent IL-7 production is distinctively regulated by expression of IL-7 transcripts that differ in their 5′ UTR. (A) Schematic drawing of human IL-7 mRNA, with the primers and cDNA probes used in this study. The nucleotide number was designated with respect to the translation start site (+1). An IRF-E located at the region from position −268 to −257 is also indicated. (B) DLD-1 and HT29-18N2 cells were stimulated with IFN-γ (50 ng/ml) for the indicated time periods. Fifteen micrograms of poly(A)$^+$ mRNA was subjected to Northern blotting for IL-7 mRNA by using the ^{32}P-labeled CS probe or the 5′ UTR probe. The bottom panel indicates the level of G3PDH mRNA as a control. (C) DLD-1 cells were treated with IFN-γ (50 ng/ml) or left untreated for 6 h, collected for total RNA isolation, and then subjected to semiquantitative RT-PCR for IL-7 mRNA. PCR amplification was performed by using either the S1, S2, or S3 primer along with AS1 primer depicted in panel A. As controls, samples from IFN-γ-treated and untreated cells were amplified with a primer set for G3PDH.

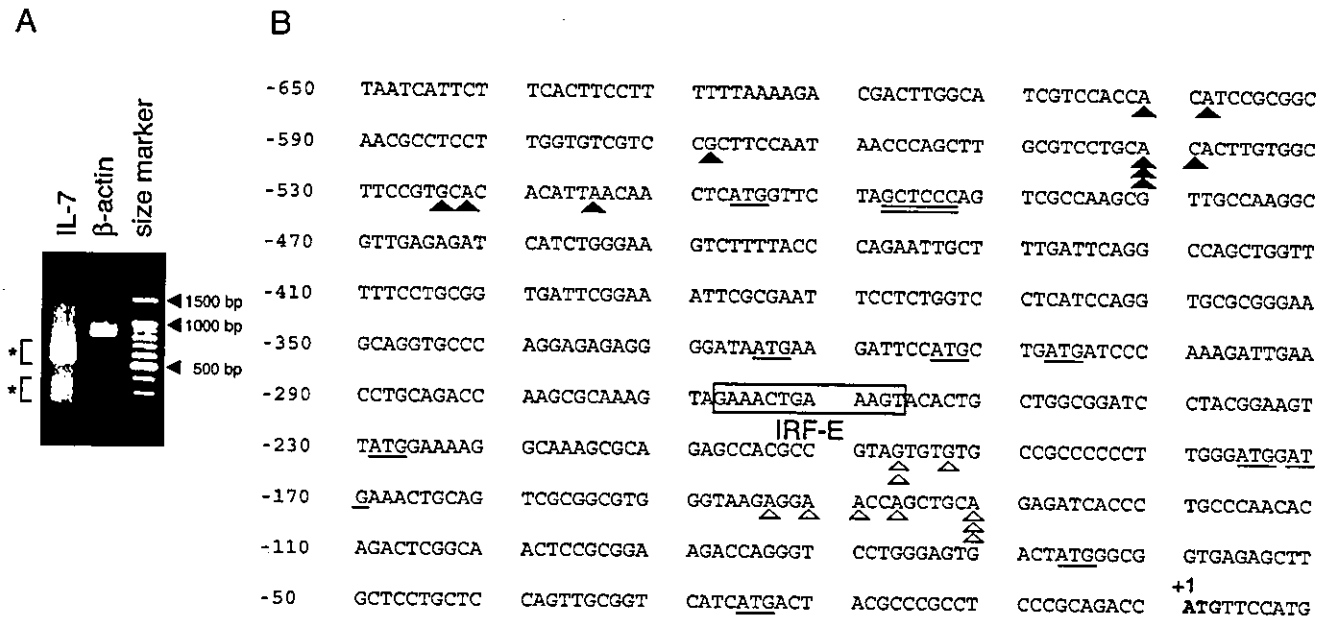

FIG. 3. Transcription initiation sites for the human IL-7 gene were clustered within two separate regions upstream from the translation start site. (A) RLM-RACE analysis was performed by using poly(A)$^+$ RNAs from IFN-γ-treated (6 h) DLD-1 cells as described in Materials and Methods. PCR products amplified by a primer set for the IL-7 or β-actin gene, respectively, were run on 1.5% agarose gel, stained with ethidium bromide, and visualized. (B) Two major fragments of ~600 and ~300 bp shown in panel A were independently cloned, and then 10 clones of each were sequenced. The 5′ end of each clone is shown by a filled triangle (clones derived from ~600-bp fragments) or an open triangle (clones from ~300-bp fragments) on the first 650 bp of sequence upstream of the translation start site. The authentic translation start site is indicated in bold. Numbering in base pairs is indicated to the left, with negative numbers representing nucleotides upstream of the ATG. Consensus sequences for the IRF-E are boxed and labeled. Potential translation initiation codons (ATG) are underlined. Consensus sequences for MED-1 are also underlined.

tempted to precisely map the 5′ end of IL-7 mRNA by using a RLM-RACE method that ensures the amplification of only full-length transcripts via the elimination of truncated mRNAs (see Materials and Methods). When poly(A)$^+$ RNA extracted from IFN-γ-treated (6 h) DLD-1 cells was analyzed, fragments around 600 and 300 bp were obtained by PCR by using the 5′ nested primer and the 3′ reverse IL-7 GSP-2 (corresponding to nucleotides 36 to 60 of the IL-7 gene) (Fig. 3A). No product was obtained when RNA was not treated with tobacco acid pyrophosphatases, indicating that these products were derived from full-length mRNA (data not shown). Both of these products appeared to migrate somewhat diffusely when subjected to gel electrophoresis (Fig. 3A). This result was not attributable to experimental artifacts, because PCR amplification with another set of primers, designed for detecting the 5′ part of the human β-actin gene, yielded products of the expected size (872 bp) that migrated as a single band from the same sample (Fig. 3A). The ~600- and ~300-bp fragments were independently isolated and cloned, and then 10 clones of each were sequenced. All 20 clones contained the IL-7 gene sequence along with the adapter sequences, showing these clones to be derived from mRNAs retaining complete 5′ ends. Alternative splicing appeared to be infrequent in this region (upstream of the sequences corresponding to IL-7 GSP-2), because no nucleotide deletion was observed in any of the sequenced clones. As depicted in Fig. 3B, the 5′ ends of longer fragments were located within the −601 to −515 region upstream of the translation start site (+1), while the 5′ ends of shorter fragments were mapped within the −197 to −131 region. These results demonstrated that the human IL-7 gene is transcribed from multiple transcription start sites that are clustered within two distinct regions approximately 300 to 500 bp apart from each other.

We then tested whether ~1.8- and ~2.4-kb IL-7 mRNAs might indeed differ in their 5′ UTR stretches by Northern blot analysis using a 5′ UTR probe corresponding to nucleotides at positions −539 to −242 (Fig. 2A). Interestingly, this probe exhibited subtle but substantial hybridization with ~2.4-kb but not with ~1.8-kb mRNA, showing the different lengths of 5′ UTR between these mRNA species (Fig. 2B). To further confirm this, RT-PCR with any of the S primers (S1, S2, or S3) along with the AS1 primer (Fig. 2A) was carried out. When RNAs from untreated and IFN-γ-treated DLD-1 cells were examined, amplification with the primer sets of S3/AS1 and S2/AS1 showed no difference in the amount of products before and after IFN-γ treatment (Fig. 2C). In contrast, amplification with the primer set of S1/AS1 displayed a significant increase in the amounts of PCR products in response to IFN-γ (Fig. 2C). Therefore, it was demonstrated that stimulation with IFN-γ preferentially induces relatively short-form IL-7 mRNA expression via the selective usage of transcription initiation sites within the region −197 to −131. Of note, the maximum difference in 5′ UTR lengths among clones obtained in RLM-RACE was less than 500 bp and did not match that between the ~2.4- and ~1.8-kb transcripts seen in Northern blot analysis. We assumed that this discrepancy might have in some part resulted from the difficulties in determining the precise size of transcripts by Northern blot analysis; however, this issue was not further examined in the present study.

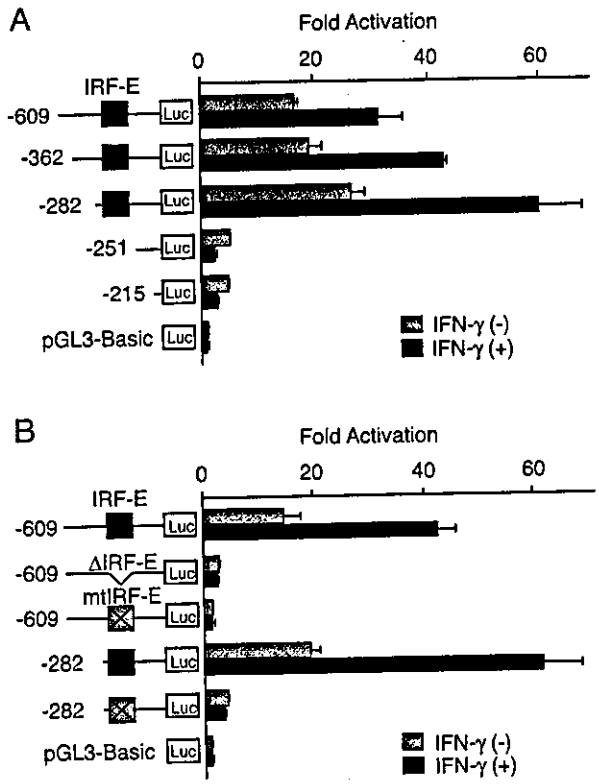

FIG. 4. IFN-γ-dependent and -independent IL-7 gene activation is mediated through IRF-E within its 5′ UTR. (A) DLD-1 cells were transiently transfected with a −609-Luc or either of its 5′ deletion mutant plasmids, cultured in the presence or the absence of IFN-γ for 12 h, and then assayed for reporter activities. (B) DLD-1 cells were transiently transfected with a −609-Luc or either of its mutated versions of plasmids, cultured as described for panel A, and then reporter activities were assayed. Luciferase activities were normalized and indicated as increases in activation compared with activity levels of cells transfected with pGL3-Basic plasmid and left untreated. Results are the means ± standard deviations of three independent experiments. Xs in boxes indicate mutated IRF-E sequences.

IFN-γ-dependent and -independent IL-7 gene expression is mediated through IRF-E within its 5′ UTR. To characterize *cis*-acting regulatory elements in the 5′ flanking or intragenic regions of the human IL-7 gene, we constructed a reporter plasmid in which the luciferase gene expression was under the control of the upstream region of the human IL-7 gene. When a reporter plasmid with the region −3194 to −3 (−3194-Luc) was transiently transfected in DLD-1 cells, a significant increase of luciferase activity was observed in both untreated and IFN-γ-treated cells, when compared to that seen with the control reporter plasmid (data not shown). A series of 5′ deletions from the −3194-Luc to position −609 (−609-Luc) showed no apparent difference in reporter activities (data not shown), and, thus, we constructed another series of 5′ deletion clones to be analyzed. As shown in Fig. 4A, the reporter activity of the −609-Luc was approximately 15-fold higher than that of the control in the absence of IFN-γ. In addition, the reporter activity exhibited approximately a twofold induction in response to IFN-γ. Deletions from the 5′ end to −282 showed a slight increase in both basal and IFN-γ-inducible reporter activities. In contrast, further deletion up to position −251 resulted in a dramatic decrease of reporter activities not only of uninduced levels but also with regard to IFN-γ-dependent induction (Fig. 4A). These results suggested that the critical enhancer element for both IFN-γ-dependent and -independent up-regulation of IL-7 gene expression might be located within the region from position −282 to −251. Substantial activities in the constitutive levels of reporter gene expression were observed further in the −215 to −3 region, while the IFN-γ-dependent induction of the reporter activity almost diminished by deleting up to position −251 (Fig. 4A). Since the region from position −282 to −251 contained an IRF-E at position −268 to −257 (Fig. 3B), we postulated that IL-7 gene activation might be mediated through this site. As expected, when an internal deletion mutant of the −282 to −251 sequence (−609-ΔIRF-E-Luc) was assayed, a drastic decrease in reporter activities in untreated as well as IFN-γ-treated cells was observed (Fig. 4B). In addition, introduction of a 4-bp mutation into the IRF-E sequences of −609-Luc and −282-Luc similarly culminated in a marked decrease in reporter activities (Fig. 4B). These findings suggested that the region from position −282 to −251 and, in particular, the IRF-E sequences within this region play a critical role in determining both IFN-γ-dependent and -independent enhancer activities in human IECs.

IRF-1 is an inducible, while IRF-2 is a constitutive, binding protein to the IRF-E. To identify nuclear factors that interact with the regulatory element of the IL-7 gene, we performed an EMSA by using a DNA probe corresponding to the sequences of the region −280 to −253. When nuclear extracts of DLD-1 and HT29-18N2 cells before and after IFN-γ addition were examined, several DNA-protein complexes were observed (Fig. 5A, C1 through C5). Among these, two (C2 and C5) displayed constitutive complex formation, and others (C1, C3, and C4) were induced by IFN-γ in both of these cell types (Fig. 5A, lanes 1 to 11). The formation of these complexes was sequence specific, since the nonlabeled DNA probe competed out the binding of nuclear proteins with the labeled probe (Fig. 5A, lane 13). In addition, a nonlabeled mutant probe did not affect complex formation, showing these complexes to be composed of proteins that specifically recognized IRF-E sequences (Fig. 5A, lane 14). Consistently, an anti-IRF-1 antibody shifted complex C3 (Fig. 5A, lanes 16 and 25), one of the inducible complexes in both cell types. In addition, complex C2, continuously observed with higher intensity in DLD-1 cells than in HT29-18N2 cells, was completely shifted with an anti-IRF-2 antibody (Fig. 5A, lanes 17 and 26). These observations were further supported by immunoblotting, since the nuclear expression of these IRF proteins correlated well with the results of the EMSA analysis (Fig. 5B). It should be noted that in the supershift experiments, nuclear complexes containing other IRF family proteins such as IRF-4, IRF-8, and IRF-9 were also present to some extent (Fig. 5A, lanes 19, 21, and 22). However, the degree of their occupancy on IRF-E sequences remained unclear, since antibodies against these molecules could neither shift nor disrupt the protein-DNA complexes. Together, these observations indicated that IRF-1 and IRF-2 bind to the IRF-E in an IFN-γ-inducible and constitutive manner, respectively, and then transcriptionally regulate IL-7 gene expression. Again, this notion showed an analogy with the previously described mechanisms of IL-7 gene transcription in

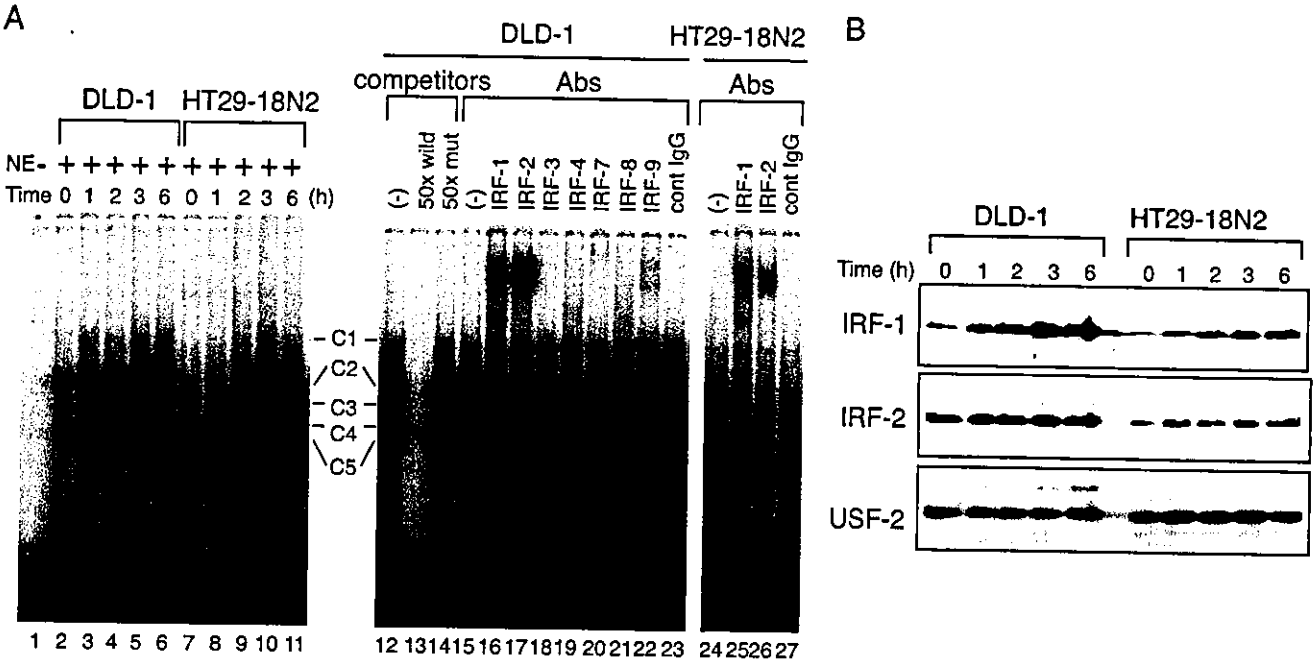

FIG. 5. IRF-1 is an inducible, while IRF-2 is a constitutive, binding protein to the IRF-E. (A) DLD-1 and HT29-18N2 cells were stimulated with IFN-γ (50 ng/ml) for the indicated time periods. Nuclear extracts (NE) were prepared, and 10 μg of each was subjected to EMSA by using ^{32}P-labeled oligonucleotide probes corresponding to the sequence −280 to −253 of the IL-7 gene (left). Competition assays were performed by adding a 50-fold molar excess of unlabeled specific oligonucleotide (wild) or the mutant (mut) probe to the reaction mixture containing the extracts from cells treated with IFN-γ for 6 h (right). Supershift assays were performed by preincubating the reaction mixture of 6 h-treated nuclear extracts with either 2 μg of antibodies (Abs) against the indicated proteins or 2 μg of mouse IgG. (B) Twenty-five micrograms of nuclear extracts as described in panel A was separated on an SDS–10% polyacrylamide gel and immunoblotted with an anti-IRF-1 antibody (IRF-1), and the blot was sequentially reprobed with an anti-IRF-2 (IRF-2), and an anti-USF-2 antibody (USF-2, loading control).

murine keratinocytes in terms of the IFN-γ-inducible DNA binding of IRF-1 to IRF-E (2). Our data, however, raised the further possibility that IRF-2, generally known as a transcriptional repressor, also acts as a positive regulator of IL-7 gene expression, since the constitutive DNA binding and relative abundance of the IRF-2-containing nuclear complex in DLD-1 compared to HT29-18N2 cells, closely paralleled the levels of IL-7 mRNA expression.

IRF-1 and IRF-2 distinctively up-regulate IL-7 protein production via IRF-E-mediated transcription. Given these observations, we next analyzed the functional effects of IRF-1 and IRF-2 on IL-7 gene expression. To this end, a −609-Luc plasmid was cotransfected with an expression plasmid for either IRF-1 or IRF-2 into DLD-1 cells. Intriguingly, introduction of not only IRF-1 but also IRF-2 significantly enhanced the reporter activities (Fig. 6A). The effects of these IRF proteins were mediated via IRF-E, since neither IRF-1 nor IRF-2 affected gene expression from a mutant reporter plasmid (Fig. 6A). These results clearly showed that both IRF-1 and IRF-2 positively regulate expression of the IL-7 gene through IRF-E on its 5′ UTR.

To examine whether such transcriptional regulation leads to IL-7 protein production, we next assessed DLD-1-derived cells in which a gene encoding either IRF-1 or IRF-2 was stably transfected. Since several studies showed that IRF-1 suppresses and that IRF-2 promotes cellular proliferation, respectively (10), we employed the TET-on inducible system to achieve conditional expression of these IRF proteins, thereby excluding the possibilities that such growth-regulating functions might affect the direct effects of IRF-mediated transcription. In our system, tagged IRF proteins were expressed upon the addition of DOX, which relieved the repressive effects of TR proteins. When each clone of DLD-1/TR/IRF-1-tag or DLD-1/TR/IRF-2-tag cells was examined, each IRF protein was efficiently induced upon DOX treatment (Fig. 6B). In addition, when analyzed by transient transfection of −609-Luc, both clones displayed marked enhancement of reporter activities in response to DOX, suggesting that these tagged IRF proteins are transcriptionally competent (data not shown). When the culture supernatants of these cells before and after the DOX addition were assayed for IL-7 by ELISA, a marked induction of IL-7 proteins was observed in both DLD-1/TR/IRF-1-tag and DLD-1/TR/IRF-2-tag cells but not in parental DLD-1 cells (Fig. 6C), indicating that activation of IRF-1 or IRF-2 could induce IL-7 protein production. We further took advantages of this system to examine how inducible expression of each IRF protein influences the profile of IL-7 mRNAs. Interestingly, when Northern blotting with the IL-7 CS probe was performed, DOX-dependent IRF-1 expression exclusively induced generation of ~1.8-kb IL-7 mRNA (Fig. 6D). In contrast, the expression of IRF-2 significantly enhanced the expression of both ~2.4- and ~1.8-kb IL-7 transcripts (Fig. 6D). These results not only demonstrated the up-regulatory functions of IRF-1 and IRF-2 on IL-7 gene expression but also further reinforced our hypothesis that IRF-1 is an inducible, while IRF-2 is a constitutive, regulator of IL-7 gene expression; that is, these data coincided with the observation that IFN-γ-dependent IRF-1 expression was followed by the predominant

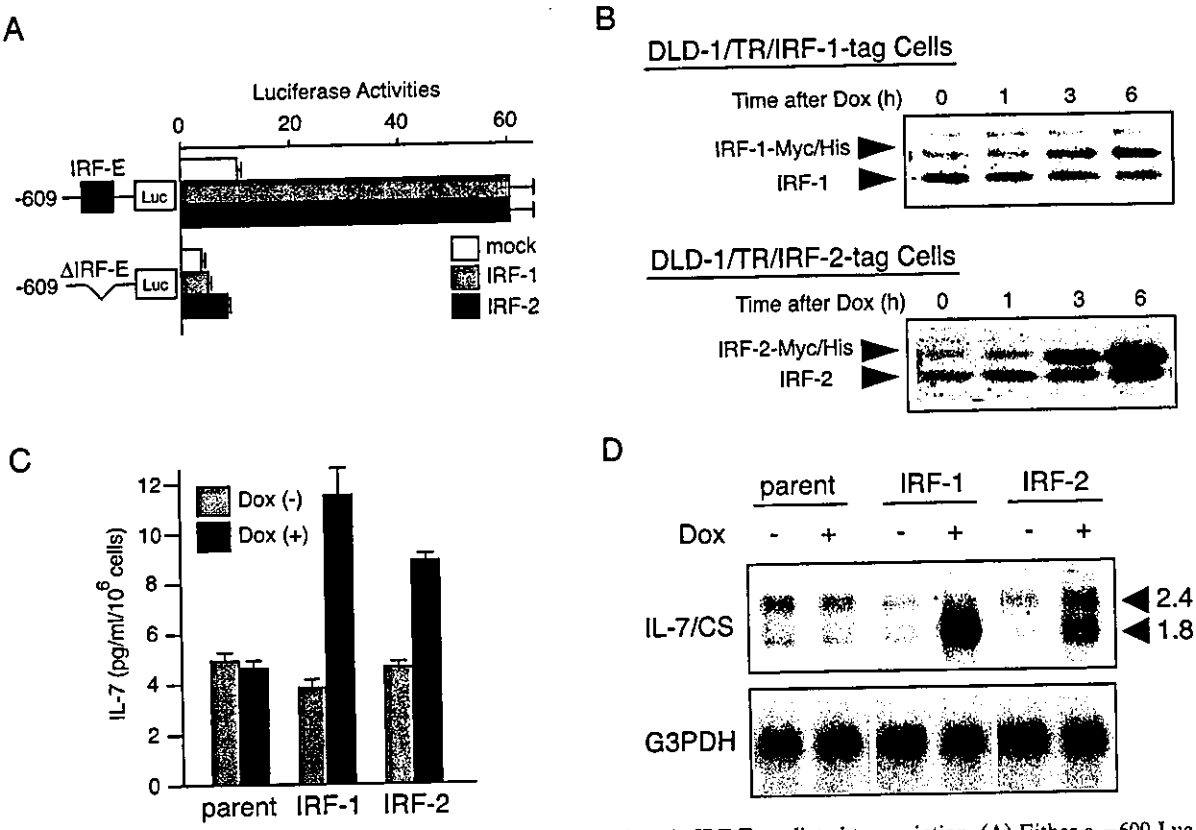

FIG. 6. IRF-1 and IRF-2 distinctively up-regulate IL-7 protein production via IRF-E-mediated transcription. (A) Either a −609-Luc plasmid or −609-mtIRF-E-Luc was transiently transfected into DLD-1 cells with 0.1 μg of the expression vector encoding either IRF-1 or IRF-2 (pcDNA3-IRF-1 or-IRF-2) or with an empty vector (mock). Cells were then cultured for 12 h and assayed for reporter activities. Luciferase activities were normalized and indicated as the means ± standard deviations of three independent experiments. (B) DLD-1-derived cells in which either IRF-1-tag or IRF-2-tag protein is inducible upon DOX were established. DLD-1/TR/IRF-1-tag and DLD-1/TR/IRF-2-tag cells were treated with DOX (100 ng/ml) for the indicated time periods. Nuclear extracts were prepared, and 25 μg of each was subjected to immunoblot analysis by using either anti-IRF-1 antibody for DLD-1/TR/IRF-1-tag cells or anti-IRF-2 antibody for DLD-1/TR/IRF-2-tag cells, respectively. (C) Parental DLD-1 (parent), DLD-1/TR/IRF-1-tag (IRF-1) and DLD-1/TR/IRF-2-tag (IRF-2) cells were treated with 100 ng of DOX (+) per ml or left untreated (−) for 24 h, and the supernatant was assayed for IL-7 production by ELISA. Results are the means ± standard deviations of three independent experiments. (D) Parental DLD-1 (parent), DLD-1/TR/IRF-1-tag (IRF-1) and DLD-1/TR/IRF-2-tag (IRF-2) cells were treated with DOX (100 ng/ml) and then collected at the time point of the addition (−) of IFN-γ or 6 h (+) after stimulation. Poly(A)$^+$ mRNA was extracted, and Northern blotting of IL-7 mRNA was performed as described in the legend of Fig. 2B by using a ^{32}P-labeled CS probe.

expression of ~1.8-kb IL-7 mRNA, whereas constitutive IRF-2 expression was accompanied with the expression of both sizes of transcripts (Fig. 2B).

Inducible and constitutive IL-7 production is suppressed by siRNAs for IRF-1 and IRF-2, respectively. To clarify the distinct roles of IRF-1 and IRF-2 in IL-7 production directly, we designed siRNAs for either of these IRFs and then examined how these siRNAs affect IL-7 production. When DLD-1 cells were transiently transfected with either of the siRNAs, IFN-γ-dependent expression levels of IRF-1 and constitutive levels of IRF-2 were suppressed by 50 and 80% at the protein levels, respectively (Fig. 7A). In parallel, in cells treated with siRNA for IRF-1, IFN-γ-dependent IL-7 production was significantly inhibited by 50%, whereas constitutive IL-7 secretion was barely affected (Fig. 7B). In striking contrast, basal levels of IL-7 protein production in cells depleted of IRF-2 by specific siRNA were reduced by 40%, while these cells displayed an efficient induction of IL-7 secretion in response to IFN-γ (Fig. 7B). These data clearly demonstrated that IRF-1 functions as an inducible factor for IL-7 production, primarily in response to cellular stimuli such as IFN-γ, while IRF-2 predominantly serves as a factor that maintains the constitutive levels of IL-7 production.

IRF-1 and IRF-2 bind to the IRF-E without competition in vivo. Our data showing the distinct functions of IRF-1 and IRF-2 on gene expression and the production of IL-7 raised the question of how the binding of each IRF to the IRF-E is regulated in vivo. To examine this, ChIP assays were performed with DLD-1 cell chromatin extracts. We designed two sets of PCR primers to amplify DNA fragments corresponding to the regions −539 to −159 and +976 to +1337 (positions on the genomic sequences relative to the translation start site), respectively (Fig. 8A). The former set of primers was used to amplify a fragment containing the IRF-E [IRF-E(+)] and the latter to amplify a distal genomic fragment within the intronic sequences more than 1.2 kb downstream of the IRF-E [IRF-E(-)]. As shown in Fig. 8B, anti-IRF-1 antibody precipitated only 0.03% of the IRF-E(+) DNA in total input chromatin in the absence of IFN-γ and, upon stimulation with IFN-γ, the levels of IRF-1 occupancy in this region significantly increased

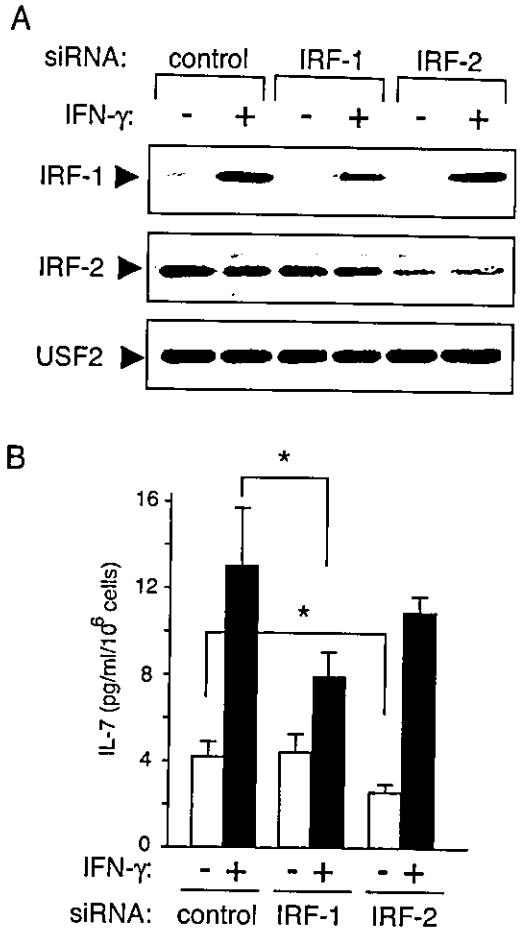

FIG. 7. Inducible and constitutive IL-7 production is suppressed by siRNAs for IRF-1 and IRF-2, respectively. DLD-1 cells were transfected with either siRNA duplex oligonucleotides targeting IRF-1, IRF-2, or control siRNA. After transfection, cells were cultured under the usual conditions for an additional 12 h, washed twice, and then cultured in the presence (+) or absence (−) of IFN-γ (50 ng/ml). The cells collected before (−) IFN-γ treatment and after 6 h (+) of IFN-γ treatment were subsequently subjected to immunoblotting (A) as described in the legend of Fig. 4B. In parallel, cells were identically treated as described for panel A, and the supernatants were collected after 24 h of culture in the presence (+) or the absence (−) of IFN-γ (B). Measurement of IL-7 was performed by ELISA, and results are indicated as the means ± standard deviations of three independent experiments. *, $P < 0.05$ by a paired Student t test.

(0.6%) (Fig. 8B). By contrast, the binding of IRF-2 to the IRF-E remained unchanged before (0.11%) and after (0.10%) stimulation with IFN-γ (Fig. 8B). The specificity of immunoprecipitation with antibodies against each IRF protein was verified by the finding that the amounts of IRF-E(+) fragments in the immunoprecipitates by control antibodies were at significantly low levels (0.02% in both IFN-γ-untreated and -treated chromatins) (Fig. 8B). In addition, specific binding of IRF-1 and IRF-2 to the IRF-E was confirmed because immunoprecipitation of IRF-1 or IRF-2 recovered only a small amount of the genomic region located far downstream of the IRF-E [IRF-E(-)], while that of histone H3 recovered approximately 10% of the total input IRF-E(-) fragments (Fig. 8B). Since there may exist variations in cross-linking and immunoprecipitation efficiency between these IRF proteins, it seems difficult to directly compare the absolute levels of promoter occupancy of these IRFs. However, from these observations, it was formally suggested that IRF-Es on the IL-7 genes are constitutively but not fully occupied by IRF-2, regardless of the

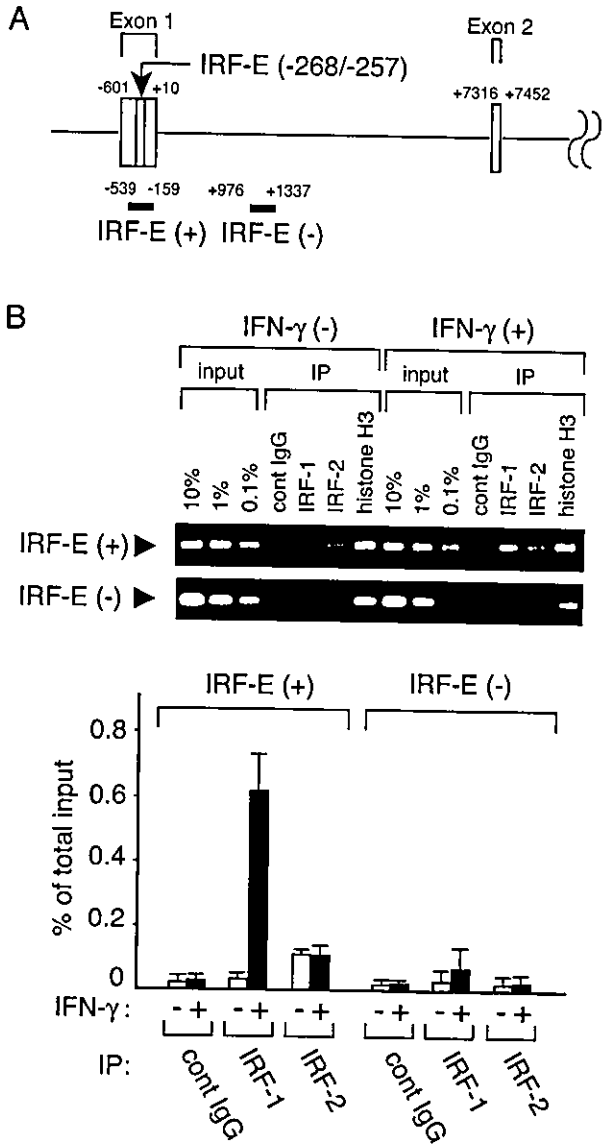

FIG. 8. IRF-1 and IRF-2 bind to IRF-E without mutual exclusion in vivo. (A) Schematic representation of the 5′ part of the human IL-7 gene. Exon 1, 2, and the intervening intron are shown with the nucleotide number relative to the translation initiation site (+1). IRF-E located in exon 1 (shaded) and the DNA regions analyzed by ChIP assays [IRF-E(+) and IRF-E(-)] are also indicated. (B) DLD-1 cells were treated with IFN-γ or left untreated for 6 h and processed for ChIP assays by using anti-IRF-1, anti-IRF-2, and anti-histone H3 antibodies (positive control) or control Ig (negative control). Precipitated DNA was subjected to both conventional PCR (top) and quantitative PCR (bottom) to amplify either the IL-7 gene fragment (−539 to −159) containing the IRF-E on its 5′ UTR [IRF-E(+)] or the intronic fragment (+976 to +1337) [IRF-E(-)]. The amount of immunoprecipitated IL-7 gene fragment relative to that present in total input chromatin (% of total input) was calculated as described in Materials and Methods. Data are shown as the means ± standard deviations of three independent chromatin immunoprecipitations (bottom). IP, immunoprecipitation; cont, control.

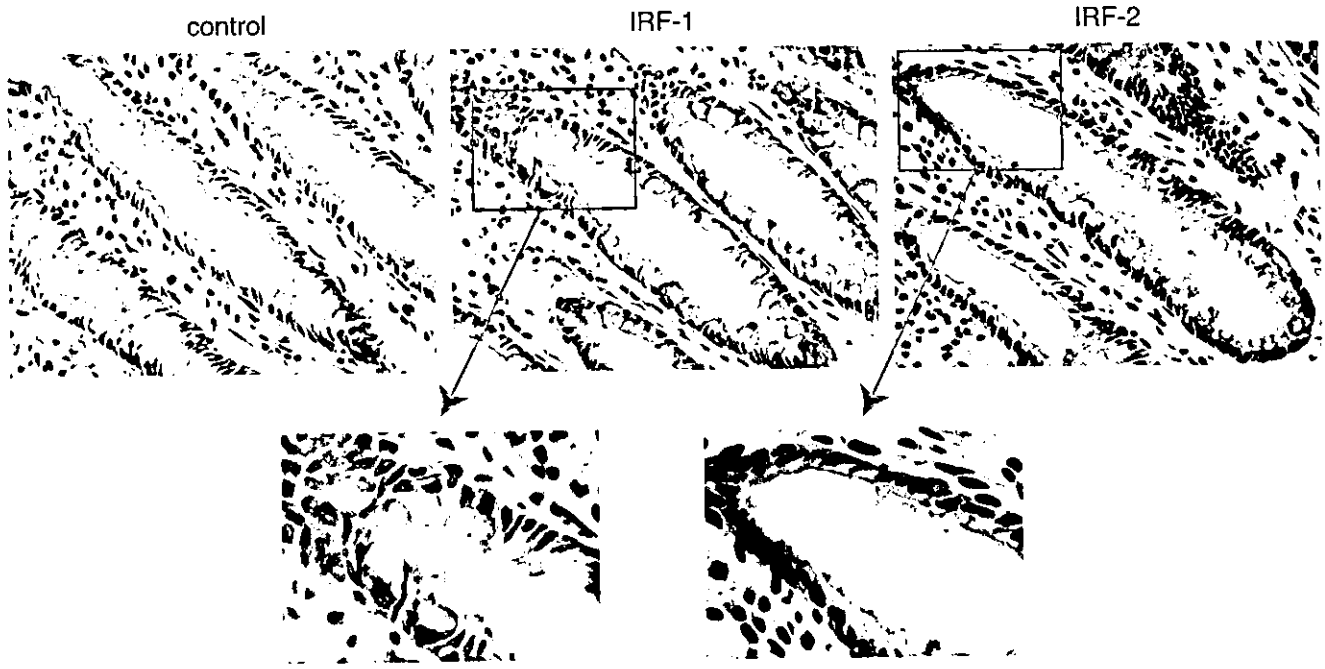

FIG. 9. IRF-1 and IRF-2 proteins are expressed in human colonic epithelial cells with distinct patterns of distribution. Sections of human colonic mucosal tissues were subjected to immunohistochemical analysis. Tissue sections (8 μm) were stained with either anti-IRF-1 (IRF-1), anti-IRF-2 (IRF-2) antibody, or purified rabbit IgG (control) (original magnification, ×400).

extracellular stimuli, and are further bound by IRF-1 upon stimulation with IFN-γ.

IRF-1 and IRF-2 proteins are expressed in human colonic epithelial cells with distinct patterns of distribution. Finally, to clarify the issue as to whether IRF-1 and IRF-2 proteins are physiologically expressed in human IECs in vivo, sections of adult human colonic tissues were immunostained with a specific antibody against IRF-1 or IRF-2. As shown in Fig. 9, both IRF proteins were expressed in colonic epithelial cells, as well as in nonepithelial cells in the lamina propria (Fig. 9). Furthermore, immunoreactivities against these factors preferentially exhibited nuclear patterns, indicating that these IRF proteins function as transcriptional regulators in human IECs in vivo. Interestingly, staining with anti-IRF-2 antibody distributed throughout the epithelial layer (Fig. 9). In contrast, IRF-1 was expressed with a patchy distribution, irrespective of the cellular configuration within the crypt (Fig. 9). Remarkably, most of the IRF-1-positive cells were shown to be epithelial goblet cells, as judged by their expanded shape at the apical portion (Fig. 9). We confirmed this finding by double staining with anti-IRF-1 antibody and acidic mucus staining with alcian blue on the same section (data not shown). These results indicated that both IRF-1 and IRF-2 proteins are expressed in colonic epithelial cells with quite distinct patterns of distribution. Moreover, together with our previous demonstration that IL-7 is substantially expressed throughout the epithelial layer, with the most abundant expression in the goblet cells (30), it was suggested that these distinct patterns of distribution might be associated with the diffuse but nonuniform expression of IL-7 in human IECs in vivo.

DISCUSSION

Recent evidence has implicated the profound effects of IL-7 on developing and mature lymphocytes not only in systemic (6) but also in local immune regulations in humans. However, the mechanisms of IL-7 production in human tissue-derived cells have remained unclear. In this study, using human IEC lines, we investigated the molecular mechanisms of IL-7 production and showed that IRF-1 and IRF-2 serve as critical factors for gene expression and the production of IL-7. Furthermore, IRF-1 and IRF-2 were demonstrated to play different roles in this process, suggesting that the IL-7 production might be regulated via finely coordinated mechanisms mediated by these IRF proteins.

Concerning the potentials of various cellular stimuli to influence IL-7 production, IL-1, TNF-α, and TGF-β had no effect and only IFN-γ was capable of regulating IL-7 production from IECs. These findings contrasted to results obtained with other tissue-derived human cells, since previous studies revealed that IL-1 and TNF-α enhance (34), while TGF-β suppresses IL-7 production in BM stromal cells (27). It seems unlikely that human IECs failed to respond to IL-1, TNF-α, or TGF-β merely due to low expression levels of the specific receptors for each factor, because most of these cytokines were proved to induce multiple biological responses within the human IEC lines or their sublines examined in this study (4, 33, 35). In addition, because the influences of these cytokines on IL-7 expression in human IECs were quite similar to those observed in murine keratinocytes (3), we favor the idea that IL-7 production in human IECs may be regulated by a tissue-specific mechanism which differs at least from that in human

BM stromal cells but resembles that in murine keratinocytes. Although the mechanisms accounting for the diversity of IL-7 production in different cell types have remained unknown, it would be of importance to clarify this issue to understand a variety of biological functions exerted by IL-7 in systemic immune regulation in humans.

In this study, we demonstrated that the transcription of the human IL-7 gene begins from multiple sites distributed within two separate regions at positions −601 to −515 and −197 to −131 bp upstream of the translation start site. Utilization of many transcription start sites is frequently observed in the regulation of genes whose promoters lack common core promoter sequences (26). Consistent with this, analysis of the human IL-7 gene revealed that none of the consensus sequences for the canonical TATA box, the initiator element YYAN(T/A)YY, or the downstream core promoter element occur within or in the vicinity of the region −601 to +1 (Fig. 3B). Instead, as initially documented in an earlier report (18), the 5′ flanking region of the human IL-7 gene displays an unusually high number of CpG dinucleotides within a ~700-bp region. This is also in accordance with the fact that a number of promoters within CpG islands lack all these classes of core elements (26). In addition, recent studies identified a new class of promoter motif on several genes that utilize multiple start sites in their TATA-less promoters. This motif, called MED-1 (multiple start site element downstream), was defined as the sequence GCTCC(C/G) and was shown to lie 20 to 45 bp downstream of the multiple transcription initiation window of various TATA-less promoters (11). Interestingly, an identical sequence to MED-1 occurs on the human IL-7 gene at position −498 (Fig. 3B), 17 to 103 bp downstream of one of two separate windows of the IL-7 gene transcription start sites. The functional relevance of these promoter structures to the start site selection of the IL-7 gene has remained undetermined; however, our work provides evidence that the expression of human IL-7 is regulated through a unique and unusual promoter architecture.

In addition to the promoter structure, unusual features of regulatory mechanisms were also found in IL-7 gene transcription. We showed that, by use of TET-inducible expression systems for each IRF protein, IRF-1 selectively induces transcription of the IL-7 gene from the relatively downstream region, while IRF-2 up-regulates transcription from two regions both upstream and downstream of IRF-E. These results suggest that utilization of the aforementioned two separate promoters is regulated by distinct as well as overlapping properties of IRF-1 and IRF-2 via binding to the same IRF-E. Recently, growing evidence has revealed the existence of alternative promoters on various human genes, suggesting the regulatory roles of alternative promoter usages in tissue-specific or developmentally controlled gene expression (15). Among these, however, the mechanism of IL-7 gene regulation seems to be unique, because there has been no report of such a gene whose alternative promoter usage is regulated by the differential binding of transcription factors to a single *cis*-element so far. At this time, it remains unclear why IRF-2 simultaneously promotes transcription from two regions but IRF-1 does not. One possible explanation for the IRF-2-mediated dual promoter usage is that the binding of IRF-2 to the IRF-E might alter the chromatin architecture to a more relaxed configuration than that of IRF-1. For example, it was shown that the proto-oncogene c-*myc* is transcribed from two distinct promoters that are located 160 bp apart, and an element called ME1a1, located between these two promoters, is required for the simultaneous opening of the chromatin configuration for both promoters (1). Therefore, it could be speculated that the IRF-E, like ME1a1 on the c-*myc* gene, might allow the transcription from two promoters only when it is bound by IRF-2 in conjunction with the specifically assembled transcription machinery.

Despite the alternative promoter usage, no variation in the resulting IL-7 proteins has been reported. Interestingly, as is the case with the murine IL-7 transcripts (8), human transcripts contain multiple potential initiation codons (nine in total throughout the −601 to −1 region) upstream from the authentic initiation codon (Fig. 3B). As these potential upstream sites generally decrease the translational efficiency (14) and as the removal of the 5′ noncoding sequence improves the translational efficiency of murine IL-7 mRNA (23), it is postulated that the human IL-7 transcripts with a shorter 5′ UTR might also be translationally more active than a transcript with a longer one.

In the present study, we demonstrated the physiological roles of IRF-1 and IRF-2 in IL-7 production by human IECs. IRF-1, originally identified as a transcriptional regulator for the human IFN-β gene (19), is induced upon various stimuli and activates target gene expression (9, 19). Likewise, we here showed that nuclear expression of IRF-1 and its binding to the IRF-E were also induced upon IFN-γ treatment in human IECs. These data recapitulated the mechanisms existing in murine keratinocytes, since it was shown that IFN-γ-dependent IL-7 gene expression was preceded by increased binding of IRF-1 to the IRF-E in these cells, and the inhibition of IRF-1 mRNA expression by UV light suppressed this IFN-γ-inducible IL-7 expression (2). In addition, our observations of DOX-inducible expression and siRNA-mediated suppression of IRF-1 were of importance, since these confirmed that such IRF-1-mediated transcription is indeed important for the inducible production of IL-7 protein. IRF-1 protein is substantially expressed with a patchy distribution in normal human intestinal epithelia, and the predominant expression of IRF-1 in goblet cells was consistent with the fact that relatively abundant expression of IL-7 is observed in these cells (30). Considering that IFN-γ is constitutively expressed in IELs (16), IRF-1 expression in vivo might be the result of the IFN-γ action that is locally produced from a certain type of cells such as IELs. Alternatively, expression of IRF-1 might be additionally regulated by stimuli other than IFN-γ, since IRF-1 is up-regulated by a variety of cellular stimuli such as various cytokines (7) and viral infection (19). At present, it is unclear which type of stimuli is responsible for IRF-1 expression in vivo and why goblet cells are prone to express IRF-1 proteins. However, our study provides not only the molecular basis accounting for the cell type-dependent variable expression of IL-7 in human IECs but also a clue for the better understanding of a well-coordinated network system within the intestinal mucosa: IL-7 production from IECs is regulated by sensing and responding to the immunological status such as the microenvironmental cytokine milieu, primarily utilizing IRF-1 as a transcriptional activator.

Although IRF-2 was originally described as a transrepressor with its potential for competing with IRF-1 (9), studies have shown that IRF-2 also functions as a transcriptional activator for several genes (12, 17, 28, 36). We here demonstrated that IRF-2 also acts as a transactivator for the IL-7 gene, but its up-regulatory functions in the production of IL-7 is quite different from those of IRF-1. Silencing IRF-2 expression by its specific siRNA resulted in suppression not of the IFN-γ-inducible but of the basal levels of IL-7 production, and DOX-regulated expression of IRF-2 enhanced IL-7 protein production via expression of both ~2.4- and ~1.8-kb IL-7 mRNAs that are constitutively expressed. Concerning the fact that IRF-2 was ubiquitously expressed throughout the epithelial layer of human colonic tissues, these findings strongly suggest that IRF-2, in contrast to IRF-1, serves as a critical regulator for IL-7 production from wide-ranging areas of human IECs in vivo. Furthermore, it was previously shown that IRF-1 is a short-lived protein with a half-life of about 30 min, while IRF-2 protein has a relatively longer half-life of more than 8 h (32). Given this, we may postulate that IRF-1 might act as a transient regulator of IL-7 production in response to cellular stimuli and, in contrast, that IRF-2 might serve as a critical factor to ensure the basal and steady-state levels of IL-7 production, not only at the cellular level but also in the tissue configuration within human intestinal mucosa.

We have previously reported that intestinal inflammation occurred in IL-7 transgenic mice (31). These mice spontaneously developed acute colitis at 1 to 3 weeks of age, which was followed by a chronic phase of colitis that histopathologically mimicked the human inflammatory bowel diseases. In these diseased mice, expression of IL-7 was increased in the acute phase while it was decreased in the chronic phase of colitis at the sites of inflammation (31). These results suggested that aberrant production of IL-7 might directly lead to the dysregulation of the local immune network in the intestinal mucosa. Based on these observations, the present study also raises the issue of a potential role of IRF proteins in human diseases such as inflammatory bowel disease. We indicated that physiological expression of IRF-1 in vivo was dominated in epithelial goblet cells, depletion of which is one of the most prominent features of ulcerative colitis in humans. Meanwhile, it is well known that the inflamed mucosa in Crohn's disease exhibit increased levels of proinflammatory cytokines including IFN-γ (25). Therefore, it is possible for us to speculate that functional alteration or a decrease in the number of goblet cells in ulcerative colitis or the altered local cytokine milieu in Crohn's disease might lead to the escape from appropriate function or expression of these IRF proteins in IECs, linking improper production of IL-7 to the dysregulation of mucosal lymphocytes within the sites of inflammation.

In summary, we here show that IRF-1 and IRF-2 serve as activators for IL-7 gene expression and protein production, while their respective roles are quite different. These results not only provide a molecular basis for understanding the profound functions of IEC-derived IL-7 in human intestinal mucosa but also suggest that the functional interplay between IRF-1 and IRF-2 is an exquisite mechanism that regulates the timely as well as continuous production of IL-7. We believe that the present work raises several interesting issues for further studies on the biological and pathological significance of these IRF proteins, especially in human IECs, in terms of their relationship with the pleiotropic functions of IL-7 in intestinal immune regulation.

ACKNOWLEDGMENTS

This study was supported in part by grants-in-aid for Scientific Research, Scientific Research on Priority Areas, Exploratory Research, and Creative Scientific Research from the Japanese Ministry of Education, Culture, Sports, Science and Technology; the Japanese Ministry of Health, Labor and Welfare; the Japan Medical Association; the Foundation for Advancement of International Science; Terumo Life Science Foundation; Ohyama Health Foundation; Yakult Bio-Science Foundation; and the Research Fund of Mitsukoshi Health and Welfare Foundation.

REFERENCES

1. **Albert, T., J. Wells, J. O. Funk, A. Pullner, E. E. Raschke, G. Stelzer, M. Meisterernst, P. J. Farnham, and D. Eick.** 2001. The chromatin structure of the dual c-myc promoter P1/P2 is regulated by separate elements. J. Biol. Chem. **276**:20482–20490.
2. **Aragane, Y., A. Schwarz, T. A. Luger, K. Ariizumi, A. Takashima, and T. Schwarz.** 1997. Ultraviolet light suppresses IFN-gamma-induced IL-7 gene expression in murine keratinocytes by interfering with IFN regulatory factors. J. Immunol. **158**:5393–5399.
3. **Ariizumi, K., Y. Meng, P. R. Bergstresser, and A. Takashima.** 1995. IFN-gamma-dependent IL-7 gene regulation in keratinocytes. J. Immunol. **154**: 6031–6039.
4. **Bartke, T., D. Siegmund, N. Peters, M. Reichwein, F. Henkler, P. Scheurich, and H. Wajant.** 2001. p53 upregulates cFLIP, inhibits transcription of NF-kappaB-regulated genes and induces caspase-8-independent cell death in DLD-1 cells. Oncogene **20**:571–580.
5. **Bilenker, M., A. I. Roberts, R. E. Brolin, and E. C. Ebert.** 1995. Interleukin-7 activates intestinal lymphocytes. Dig. Dis. Sci. **40**:1744–1749.
6. **Fry, T. J., and C. L. Mackall.** 2002. Interleukin-7: from bench to clinic. Blood **99**:3892–3904.
7. **Fujita, T., L. F. Reis, N. Watanabe, Y. Kimura, T. Taniguchi, and J. Vilcek.** 1989. Induction of the transcription factor IRF-1 and interferon-beta mRNAs by cytokines and activators of second-messenger pathways. Proc. Natl. Acad. Sci. USA **86**:9936–9940.
8. **Goodwin, R. G., S. Lupton, A. Schmierer, K. J. Hjerrild, R. Jerzy, W. Clevenger, S. Gillis, D. Cosman, and A. E. Namen.** 1989. Human interleukin 7: molecular cloning and growth factor activity on human and murine B-lineage cells. Proc. Natl. Acad. Sci. USA **86**:302–306.
9. **Harada, H., T. Fujita, M. Miyamoto, Y. Kimura, M. Maruyama, A. Furia, T. Miyata, and T. Taniguchi.** 1989. Structurally similar but functionally distinct factors, IRF-1 and IRF-2, bind to the same regulatory elements of IFN and IFN-inducible genes. Cell **58**:729–739.
10. **Harada, H., M. Kitagawa, N. Tanaka, H. Yamamoto, K. Harada, M. Ishihara, and T. Taniguchi.** 1993. Anti-oncogenic and oncogenic potentials of interferon regulatory factors-1 and -2. Science **259**:971–974.
11. **Ince, T. A., and K. W. Scotto.** 1995. A conserved downstream element defines a new class of RNA polymerase II promoters. J. Biol. Chem. **270**:30249–30252.
12. **Jesse, T. L., R. LaChance, M. F. Iademarco, and D. C. Dean.** 1998. Interferon regulatory factor-2 is a transcriptional activator in muscle where it regulates expression of vascular cell adhesion molecule-1. J. Cell Biol. **140**: 1265–1276.
13. **Kanamori, Y., K. Ishimaru, M. Nanno, K. Maki, K. Ikuta, H. Nariuchi, and H. Ishikawa.** 1996. Identification of novel lymphoid tissues in murine intestinal mucosa where clusters of c-kit+ IL-7R+ Thy1+ lympho-hemopoietic progenitors develop. J. Exp. Med. **184**:1449–1459.
14. **Kozak, M.** 1984. Selection of initiation sites by eucaryotic ribosomes: effect of inserting AUG triplets upstream from the coding sequence for preproinsulin. Nucleic Acids Res. **12**:3873–3893.
15. **Landry, J. R., D. L. Mager, and B. T. Wilhelm.** 2003. Complex controls: the role of alternative promoters in mammalian genomes. Trends Genet. **19**: 640–648.
16. **Lundqvist, C., S. Melgar, M. M. Yeung, S. Hammarstrom, and M. L. Hammarstrom.** 1996. Intraepithelial lymphocytes in human gut have lytic potential and a cytokine profile that suggest T helper 1 and cytotoxic functions. J. Immunol. **157**:1926–1934.
17. **Luo, W., and D. G. Skalnik.** 1996. Interferon regulatory factor-2 directs transcription from the gp91phox promoter. J. Biol. Chem. **271**:23445–23451.
18. **Lupton, S. D., S. Gimpel, R. Jerzy, L. L. Brunton, K. A. Hjerrild, D. Cosman, and R. G. Goodwin.** 1990. Characterization of the human and murine IL-7 genes. J. Immunol. **144**:3592–3601.
19. **Miyamoto, M., T. Fujita, Y. Kimura, M. Maruyama, H. Harada, Y. Sudo, T. Miyata, and T. Taniguchi.** 1988. Regulated expression of a gene encoding a